NACA TN 2354

NATIONAL ADVISORY COMMITTEE FOR AERONAUTICS

TECHNICAL NOTE 2354

A NUMERICAL APPROACH TO THE INSTABILITY PROBLEM OF MONOCOQUE CYLINDERS

By Bruno A. Boley, Joseph Kempner and J. Mayers

Polytechnic Institute of Brooklyn

NACA

Washington

April 1951

DISTRIBUTION STATEMENT A
Approved for Public Release
Distribution Unlimited

Reproduced From
Best Available Copy

20000816 144

AQM00-11-3556

NATIONAL ADVISORY COMMITTEE FOR AERONAUTICS

TECHNICAL NOTE 2354

A NUMERICAL APPROACH TO THE INSTABILITY PROBLEM OF MONOCOQUE CYLINDERS

By Bruno A. Boley, Joseph Kempner
and J. Mayers

SUMMARY

Two closely related numerical methods which employ operations tables have been developed and used in the calculation of the buckling load of a monocoque cylinder subjected to pure bending. They are based on the assumption of a simplified structure which includes only the most highly compressed portion of the cylinder. The first method makes use of a 14-row determinant, whereas the second method requires the solution of a single 10-row determinant. The buckling loads of three cylinders with widely different characteristics were calculated by these methods. Reasonable agreement with experiment was obtained.

A procedure similar to the first method was developed for the calculation of the buckling load of a cylinder with a cutout. A limited experimental check was obtained.

INTRODUCTION

The calculation of the buckling loads of reinforced monocoque cylinders is a problem of some importance in airplane stress analysis. Existing theoretical methods for determining such buckling loads, including energy methods, are, in general, lengthy and difficult to apply. A numerical procedure is therefore developed in this report in order to simplify the calculations.

Southwell's relaxation procedure (reference 1) and, in general, methods which make use of an operations table (see appendix A) have been successful in the solution of a variety of stress-distribution problems. It was therefore natural that an attempt be made to adapt these methods to buckling-load calculations. In reference 2 three closely related methods for determining the buckling load from an operations table were established and described. A limited experimental check was also obtained. In reference 2 the three methods were called the Determinant, Energy, and Convergence Methods. In this paper, the first two of these methods, along

with slight modifications, are used to calculate the buckling load in pure bending of four monocoque cylinders with widely different characteristics, one of which had a symmetric cutout on the compression side. It was found that the buckling loads could be conveniently calculated when the actual cylinder was replaced by a simplified structure preserving the main characteristics of the original cylinder.

A twofold purpose is thus fulfilled by this investigation. In the first place, a method which is fairly short and reasonably accurate is developed for the calculation of the buckling load of a monocoque cylinder. Secondly, a further experimental check of the methods of reference 2 is afforded by a comparison of the theoretical and experimental buckling loads for the cylinders considered.

The authors are indebted to Dr. N. J. Hoff for his advice and helpful criticism, and to Messrs. J. Mele, B. Erickson, and E. B. Beck for their part in the experimental phase of the investigation. The work was sponsored by and conducted with financial aid from the National Advisory Committee for Aeronautics.

CALCULATION OF BUCKLING LOAD OF CYLINDERS WITHOUT CUTOUT

Methods of Calculation

The buckling loads were calculated for three cylinders, the characteristics of which are given in table I and figure 1. The methods of calculation which appeared most convenient are described below. These methods yield the load P in the most highly compressed stringer at the instant of buckling of the cylinder as a whole. From this load the total applied bending moment can be calculated, provided the stress distribution is known. The validity and the accuracy of the methods are discussed in the next section. Basic theoretical considerations underlying the calculations may be found in reference 2 and in appendix A. A numerical example is given in appendix B.

Simplified-cylinder solution.- Let the cylinder under consideration be replaced by the simplified structure of figure 2. The operations table corresponding to this structure is that presented in table II. All symbols which appear in this table are defined in appendix C. It should be noticed that the operations table is symmetrical about its main diagonal. The buckling load P has the value which will make the determinant represented by table II equal to zero. It may be most conveniently obtained by evaluating numerically the determinant for several values of P, plotting the determinant values against P, and reading off the load at which the determinant is zero. If the load P is lower than the first buckling

load, the determinant will be positive (because it contains an even number of rows; see reference 2). If the determinants are evaluated by the method of reference 3, that portion of the so-called "auxiliary matrix" which corresponds to the first nine rows of table II need be considered only once, since it is independent of the load P.

Solution with assumed displacements.- The above method can be simplified by assuming the following expressions for the radial displacements r and the rotations m_t of the most highly compressed stringer (stringer 1, fig. 2):

$$\left.\begin{aligned} r &= \sin^5(\pi x/6L) \\ m_t &= (dr/dx) = (5\pi/6L)\sin^4(\pi x/6L)\cos(\pi x/6L) \end{aligned}\right\} \quad (1)$$

in which the maximum radial displacement is taken as unity, and L is the ring spacing. At rings B, C, and D, respectively (see fig. 2), x = L, 2L, and 3L. The determinant is then reduced to that given in table III. In the presentation of this table advantage was taken of symmetry. The buckling load may be obtained from this determinant by the first method given above. Since, however, only the element in the lower right-hand corner is a function of the load P, the determinant will take the form $[K + f(kL)]$, where K is a constant not dependent on P,

$$k = \sqrt{P/(EI)_{str_r}} \quad (2)$$

f(kL) is given in table III, and $(EI)_{str_r}$ is the radial bending rigidity of the stringer and its effective width of sheet. The value of kL at buckling makes the determinant vanish and may be obtained from the equation

$$f(kL) = -K \quad (3)$$

A curve of f(kL) against kL is given in figure 3 and may be used to solve this equation in a convenient manner. Consequently the buckling load of a cylinder can be obtained from the solution of a single 10-row determinant.

It is useful to note than an upper and lower limit may be found for the value of kL at buckling, such that

$$1.46 < kL < 4.49$$

The value 4.49 corresponds to the lowest load at which a main-diagonal element (in the tenth or eleventh rows) of table II becomes zero. The value 1.46 is the value at which $f(kL) = 0$ and is approximate since it depends on the assumption of equations (1).

It may be noticed that both methods require the evaluation of at least one determinant. It is suggested that this evaluation be carried out by the method of reference 3. The following remarks concerning the application of this method in the present problem may be useful:

(1) The operations table is symmetric about its main diagonal

(2) The value of the determinant is equal to the product of the main-diagonal elements of the auxiliary matrix (defined in reference 3)

(3) The determinant will be equal to zero when the last main-diagonal element of the auxiliary matrix vanishes (see appendix A)

Discussion of Methods

The methods outlined in the preceding section are based on the simplified structure of figure 2. The following considerations underlie the choice of this structure and of the methods of calculation:

(1) The most highly compressed stringer was considered of paramount importance at buckling, so that it was thought permissible to neglect all other stringers in these approximate calculations. This is equivalent to considering the most highly compressed stringer as a column elastically supported by the rings and sheet. The elasticity of the supports is represented by the ring and sheet influence coefficients in the operations table (appendix B).

(2) Points on the tension side of the cylinder will undergo only negligible displacements and hence may be considered fixed. The rings are therefore assumed to continue up to a point, near the tension side, 90° away from the most highly compressed stringer, and to be rigidly fixed there (fig. 2).

(3) It would seem natural to continue the sheet up to the same point as the rings. Because all stringers except the most highly compressed one have been neglected, this would imply a single panel of sheet in each bay, extending over 90°. The operations table, however, is set up considering each panel with its edge reinforcements as a unit in which only the corner points have independent freedom of motion (see, e.g., reference 4). Therefore the action of the 90° sheet panel would be determined by the displacements of its corners, with no possibility of

intermediate adjustment. Consequently the rigidity of the panel would be greatly exaggerated. The decrease in the effective shear modulus of the buckled sheet (reference 5) because of the larger angle subtended would not provide a sufficient reduction in the shear rigidity. The sheet panel was therefore taken to be smaller, the natural stopping point being the position of the stringer next to the most highly compressed stringer in the actual cylinder. Thus only the sheet which provides additional stiffness to the most highly compressed stringer is considered. This appears consistent with the assumption that all other stringers may be neglected. A point with independent freedom of motion was therefore considered in each ring at the intersection with the free edge of the sheet. It may be remarked that, if the rings were to be terminated there, the consequent reduction in the influence coefficients would in general be negligibly small.

(4) The length of the cylinder was considered constant and equal to six times the ring spacing. For the three cylinders investigated, PIBAL cylinder 10 and GALCIT cylinders 25 and 65 (fig. 1), this corresponds to 1.5, 1.5, and 1.2 times the respective diameters. For the fuselage of a large modern transport this length would be approximately equal to the diameter. The following table may be set up on the basis of experimental results presented in the references given:

Loading	Limiting value of L'/D	Increase in buckling load at lower value of L'/D (percent)	Reference
Compression	1.5	6 at $L'/D = 1.0$	6
Pure bending	2.0	12 at $L'/D = 1.2$	7

The buckling load is practically independent of the length if the length-to-diameter ratio L'/D is equal to or larger than the limiting value given. Examples of the increase in the buckling loads for cylinders shorter than the limiting length are given in the third column of the above table. The length assumed in the calculation will be in general somewhat shorter than the limiting length; the error caused by this may be estimated with the aid of the above table to be at most 10 or 15 percent of the buckling load of a cylinder longer than the limiting length. The effect of the length was investigated in some detail with test cylinder 25 of the GALCIT series (reference 8). The buckling load for this cylinder was calculated considering different numbers of bays and the results are shown in figure 4. It may be seen that the calculated buckling loads approach some constant value in what appears to be an asymptotic variation and that the difference in the buckling loads obtained considering six or eight bays is small. It was concluded that the small improvement in accuracy given by a longer structure did not warrant the increased amount of work required to obtain it.

(5) The buckling load was calculated with the aid of the simplified structure for test cylinders 25 and 65 of the GALCIT series (reference 8) and for cylinder 10 of the PIBAL series (reference 9). Those specimens were chosen because of their widely different characteristics (see fig. 1 and table I). Comparisons of the results of the present analysis with those of experiment are presented in table IV and in figures 4, 5, and 6. The calculated buckling loads may be seen to be consistently higher than the corresponding experimental values. The percentage errors obtained are not considered excessive, however, upon comparison with the results obtained earlier at PIBAL by means of strain-energy methods. One of those solutions (reference 10) gave better results than the present investigation, but required a prohibitive amount of work.

(6) Approximate deflected shapes at buckling obtained with the aid of the simplified structure of figure 2 are given in table V for the three cylinders investigated. The same table also gives results of measurements made on some actual test specimens after buckling (reference 6). It may be noticed that fair agreement has been obtained between measured and calculated values, so that an additional indirect experimental check has been provided on the reasonableness of the simplified structure chosen. It should be kept in mind that the measurements were taken after the cylinders had buckled, and therefore may differ from the actual displacements at the instant of buckling.

(7) Table V also shows that the radial displacements r of the most highly compressed stringer at buckling are closely represented by

$$r = \sin^n(\pi x/6L) \tag{4}$$

where $n = 4$, 5, or 6. The rotations m_t may be closely approximated by

$$m_t = (n\pi/6L) \sin^{n-1}(\pi x/6L) \cos(\pi x/6L) \tag{5}$$

The values obtained with $n = 5$ represent a reasonable average of all experimental and calculated deflections, and therefore this value of n was chosen for the solution with assumed displacements which was described previously. As a check, the buckling load of GALCIT cylinder 65 was calculated by that method and was found to be 1730 pounds. The buckling load calculated from the simplified structure without the assumption of displacements was 1670 pounds (fig. 5), so that the error introduced by this assumption is only 3.6 percent of the latter value. Cylinder 65 was chosen since it is the specimen for which the agreement between assumed and actual displacements is the poorest (table V). It should be remembered in this connection that it was shown elsewhere (reference 2) that the methods of calculation used in this report are not too sensitive to errors in the assumed deflected shape.

(8) The operations tables for the simplified structure (tables II and III) may be put in nondimensional form by the following process. Divide the tenth and eleventh rows and columns by L, and all terms in rows and columns (10) through (14) by the quantity $G_{eff}td/L$. The beam-column terms appearing in the lower right-hand corner may then be written as $(EI)_{str_r}/L^3$ times some function of kL. The ring influence coefficients $\widehat{rr}$, $\widehat{rm}$, $\widehat{rt}$, and so forth are equal to $(EI)_r/d^3$ multiplied by some function of r/d (reference 11). If all rows and columns are divided through by $(EI)_r/d^3$ it will be noticed that the operations table will be a function of the four nondimensional parameters

$$\left.\begin{aligned} \Lambda &= \frac{r^4}{L^3 d}\frac{(EI)_{str_r}}{(EI)_r} \\ \Gamma &= \frac{G_{eff}td^4}{(EI)_r L} \\ &\quad r/d \\ &\quad kL \end{aligned}\right\} \qquad (6)$$

where r is the cylinder radius, $(EI)_r$ the bending rigidity of a ring in its own plane, d the circumferential stringer spacing, G_{eff} the effective shear modulus for the sheet, t the sheet thickness, and the other symbols have been previously defined. The effects of shearing and extensional deformations of the rings, respectively, are represented by the two additional parameters:

$$\left.\begin{aligned} \xi &= A_r^*/A_r \\ \gamma &= A_r d^2/I_r \end{aligned}\right\} \qquad (7)$$

where I_r is the moment of inertia of the ring cross section, A_r is the area of the ring, and A_r^* is the effective shear area of the ring cross section. Reference 11 shows, however, that the effect of these two parameters is in general negligible.

It has been shown in reference 12 that the buckling load of a monocoque cylinder depends on the parameter Λ. Two additional parameters

were established in that reference by physical reasoning to be r/d and ϵ/ϵ_{cr}, where ϵ is the strain in the most highly compressed stringer at failure and ϵ_{cr} is the buckling strain of a sheet panel. An experimental verification of the fact that these parameters approximately control the buckling phenomenon in monocoque cylinders is given in reference 13. It may be seen that two of the parameters found in the present development are the same as those found in reference 12, while the parameter Γ includes the quantity ϵ/ϵ_{cr}, since the shearing rigidity G_{eff} was found in reference 5 to be closely approximated by

$$\frac{G_{eff}}{G_0} = N + (1 - N)e^{-N\,\epsilon/\epsilon_{cr}} \tag{8}$$

where

$$N = 0.0275\left[(2\pi r/d) + 1\right] \tag{8a}$$

and G_0 is the shear modulus of the sheet material.

Curves of kL, which represents the buckling load, plotted against the parameters Λ and Γ are shown in figure 7 for all the cylinders of reference 8 with $r/d = 6.32$. An insufficient number of cylinders is available so that the position of these curves is not definitely determined. It may be stated, however, that the results presented do not contradict the validity of the four parameters established.

CALCULATION OF BUCKLING LOAD OF A CYLINDER WITH A CUTOUT

Experimental Investigation

The methods developed previously were extended to include cylinders with cutouts. A cylinder with a cutout (PIBAL cylinder 82, fig. 8), which consisted of a thin circular shell reinforced by six stringers and four evenly spaced rings was therefore constructed and tested. The cutout extended circumferentially for 90° on the compression side of the cylinder. Pure bending moments were transmitted to the ends of the cylinder through heavy rings which could be assumed rigid. The test rig was the same as that used in the cylinder tests of reference 13. This cylinder buckled when the load in the most highly compressed stringer (stringer 2 in fig. 8) was 5400 pounds. This load corresponded to a total applied moment of 158,000 inch-pounds. Photographs of the buckling cylinder are shown in figures 9 and 10.

Method of Calculation

The results of the theoretical investigation indicated that the simplified methods evolved for complete cylinders are not satisfactory for cylinders with cutouts. For such cylinders, the distortion under load depends primarily on the geometry of the cutout, so that only displacements in the vicinity of the cutout require consideration in the operations table.

With consideration of the symmetry of the cylinder, an operations table including only the displacements r_{B1} and r_{B2} and the rotation m_{tB2} (see fig. 8) was set up. The resulting buckling load was, for all practical purposes, the same as that obtained through the use of an operations table which permitted all possible generalized displacements at all the joints of the cylinder. Hence the assumption that only the joints in the vicinity of the cutout need be considered in the operations table was justified for the cylinder with a cutout. The actual experimental deflected shape of PIBAL cylinder 82 (figs. 9 and 10) shows that the major distortions took place in the vicinity of the cutout, and that all other joints may be assumed to have had zero displacements.

Cylinders encountered in practice, however, will be of a more complicated construction than PIBAL cylinder 82, and hence the simplified operations table described above may not be sufficiently complete. Depending on the size of the cutout, it is suggested that the operations table be expanded so as to include all the joints surrounding the particular cutout.

The buckling load obtained for PIBAL cylinder 82 considering only three generalized displacements was 8400 pounds. The discrepancy between the theoretical and experimental buckling loads was attributed, mainly, to the inaccuracy of the value of the effective shear modulus G_{eff} used in the calculations. This value was $0.71G_0$ and was taken from equation (8). This equation is based on tests on panels buckled because of compression. The sheet panels in the present cylinder, however, are under the action of combined compression and shear. No values for the effective shear modulus of curved panels under such a loading could be found in the literature, but, according to data obtained from flat panels (reference 14), it appears that the correct value of G_{eff} should be considerably lower. Furthermore, as is shown in the next section, there is reason to reduce the shear modulus even further.

The calculations for PIBAL cylinder 82 were therefore repeated with an assumed value of $G_{eff} = 0.1G_0$. The resulting buckling load was 5900 pounds, which may be seen to be in good agreement with experiment.

Reduced Effective Shear Modulus

If a panel of sheet is not in a buckled state, the relation between shear stress τ and shear strain γ is simply Hooke's law:

$$\tau = G_0\gamma \tag{9}$$

If the panel is in a buckled state, a relation analogous to equation (9) will still hold between the average shear stress τ_{av} and the average shear strain γ_{av}, provided that an effective shear modulus G_{eff} is used in place of G_0. In other words,

$$\tau_{av} = G_{eff}\gamma_{av} \tag{10}$$

and $G_{eff} = G_0$ if the panel is not buckled. The value of G_{eff} will represent the complex state of stress of the buckled panel, and will presumably vary with panel dimensions and type of loading.

The value of G_{eff} is the proportionality factor between the average shear stress and the average shear strain. In problems of instability, however, it is desired to know the relation between a small increase in stress $d(\tau_{av})$ and a small increase in strain $d(\gamma_{av})$. This relation will again have the same form as equation (9), if only a reduced effective shear modulus $G_{eff_{red}}$ is used in place of G_0. In other words,

$$d(\tau_{av}) = G_{eff_{red}}\, d(\gamma_{av}) \tag{11}$$

Thus this new modulus represents the resistance the panel will offer against distortions additional to those represented by γ_{av}. According to the previous discussion, this new modulus will also depend upon the dimensions of the panel and upon the amount of shearing and compressive loads present.

If equation (10) is written in differential form as

$$d(\tau_{av}) = \left[\gamma_{av}\frac{d(G_{eff})}{d(\gamma_{av})} + G_{eff}\right] d(\gamma_{av}) \tag{12}$$

comparison with equation (11) indicates that

$$G_{eff_{red}} = G_{eff} + \gamma_{av}\frac{d(G_{eff})}{d(\gamma_{av})} \tag{13}$$

The following remarks may be made about the reduced effective shear modulus $G_{eff_{red}}$:

(1) $G_{eff_{red}} = G_0$ when the panel is not in a buckled state

(2) $G_{eff_{red}} = G_{eff}$ when the average shearing strain in the panel is zero immediately before buckling

(3) $G_{eff_{red}} = G_{eff}$ when there is no change of shearing strain during buckling of the structure under consideration

(4) $G_{eff_{red}} < G_{eff}$ in all other cases, since in general the modulus G_{eff} decreases with increasing shear strain γ_{av}, so that the second term in the right-hand side of equation (13) is negative

The latter case applies to the cylinder with a cutout. The low value assumed for the shear modulus in the calculations is therefore plausible.

Polytechnic Institute of Brooklyn
Brooklyn, N. Y., August 31, 1948

APPENDIX A

BASIC THEORY

The procedures developed in this report for the calculation of the buckling load of a monocoque cylinder are based on methods developed in reference 2 which make use of an operations table similar to that used in Southwell's method of systematic relaxation. These methods are outlined here, more rigorous proofs being given in reference 2. Rigorous proofs are only given here for some modifications of these methods which were not discussed in that reference.

Consider several points in the structure in question distributed so as to cover the entire structure. Let these points be numbered consecutively from 1 to n. The generalized force exerted on joint i by a generalized displacement x_j at joint j (all joints but j being considered temporarily rigidly fixed) may be denoted by $a_{ij}x_j$. The quantity a_{ij} is called an influence coefficient. If F_i is the generalized external force acting at joint i, the equilibrium condition for the ith joint is

$$F_i + \sum_{j=1}^{n} a_{ij}x_j = 0 \tag{A1}$$

provided that the principle of superposition is valid. If equation (A1) is written for every joint in the structure, a set of linear simultaneous equations will result with generalized displacements as unknowns. The array, or matrix, of the coefficients of this set of equations is called the operations table and may be written as

$$A_n = \begin{vmatrix} a_{11} & a_{12} & \cdots & a_{1i} & \cdots & a_{1j} & \cdots & a_{1n} \\ a_{21} & a_{22} & \cdots & a_{2i} & \cdots & a_{2j} & \cdots & a_{2n} \\ \cdots & \cdots & \cdots & \cdots & \cdots & \cdots & \cdots & \cdots \\ \cdots & \cdots & \cdots & \cdots & \cdots & \cdots & \cdots & \cdots \\ a_{i1} & a_{i2} & \cdots & a_{ii} & \cdots & a_{ij} & \cdots & a_{in} \\ \cdots & \cdots & \cdots & \cdots & \cdots & \cdots & \cdots & \cdots \\ a_{j1} & a_{j2} & \cdots & a_{ji} & \cdots & a_{jj} & \cdots & a_{jn} \\ \cdots & \cdots & \cdots & \cdots & \cdots & \cdots & \cdots & \cdots \\ a_{n1} & a_{n2} & \cdots & a_{ni} & \cdots & a_{nj} & \cdots & a_{nn} \end{vmatrix} \tag{A2}$$

As a consequence of Maxwell's reciprocal theorem $a_{ij} \equiv a_{ji}$.

Equation (A1) represents the equilibrium conditions for the given structure in terms of displacements. In general, the determinant A_n will not be equal to zero; then, only one set of displacements may be found which will satisfy the equilibrium conditions. If the determinant A_n vanishes, however, more than one such set of displacements will exist. This is physically possible only at neutral equilibrium, or, which is the same, at a buckling load. This leads to what was called in reference 2 the Determinant Method, the basis of which is the fact that the lowest load at which the determinant A_n vanishes is the lowest buckling load.

A proof will now be given of the fact that in general at the lowest buckling load the last main-diagonal element of the auxiliary matrix of the method for evaluating determinants given in reference 3 is equal to zero. Let the symbol A_i stand for the determinant

$$A_i = \begin{vmatrix} a_{11} & a_{12} & \cdots & a_{1i} \\ a_{21} & a_{22} & \cdots & a_{2i} \\ \cdots & \cdots & \cdots & \cdots \\ a_{i1} & a_{i2} & \cdots & a_{ii} \end{vmatrix} \tag{A3}$$

The value of this determinant is equal to the product of the first i main-diagonal terms of the auxiliary matrix. If auxiliary-matrix elements are denoted by the symbol α_{ij}, then

$$A_i = \prod_{j=1}^{i} \alpha_{jj} = \alpha_{11}\,\alpha_{22} \cdots \alpha_{kk} \cdots \alpha_{ii} \tag{A4}$$

Let A_k be the first of these determinants to vanish; then theorem 2 of reference 2 gives

$$A_k = A_{k+1} = \cdots = A_n = 0 \tag{A5}$$

where A_n is the determinant given in equation (A2). Two cases may then be considered:

Case 1; k = n.- In the case where $k = n$, A_n is the only one of these determinants which vanishes. By equation (A4) the only factor which is contained in A_n and in no other A_i determinant is α_{nn}, which, as was to be proved, must therefore vanish.

Case 2; k < n.- In the case where $k < n$, the method of reference 3 fails to give any terms beyond α_{kk}, which of course is zero. Here α_{nn}

is obviously not the first term to vanish, but in this case several of the higher buckling loads are identical with the first. This case is expected to occur rather infrequently.

The Energy Method of reference 2 is based on the condition that the second variation of the total potential energy must vanish at buckling. This condition may be written as

$$Q = \sum_{i=1}^{n} \sum_{j=1}^{n} a_{ij} x_i x_j = 0 \tag{A6}$$

This equation is satisfied at buckling by the buckling displacements. In the Energy Method some of these displacements, say x_p, x_{p+1}, . . ., x_n, are guessed; then the others are obtained from the conditions

$$\frac{\partial Q}{\partial x_k} = 0 \qquad k = 1, 2, \ldots, p - 1 \tag{A7}$$

The matrix of the coefficients of these simultaneous equations, including the constant terms, is the reduced matrix A', where:

$$A' = \begin{vmatrix} a_{11} & a_{12} & \cdots & a_{1,p-1} & a'_{1,p} \\ a_{21} & a_{22} & \cdots & a_{2,p-1} & a'_{2,p} \\ \cdots & \cdots & \cdots & \cdots & \cdots \\ a_{p-1,1} & a_{p-1,2} & \cdots & a_{p-1,p-1} & a'_{p-1,p} \\ a'_{p,1} & a'_{p,2} & \cdots & a'_{p,p-1} & a'_{p,p} \end{vmatrix} \tag{A8}$$

in which

$$a'_{ip} = a'_{pi} = \sum_{j=p}^{n} a_{ij} x_j$$

and

$$a'_{p,p} = \sum_{i=p}^{n} \sum_{j=p}^{n} a_{ij} x_i x_j$$

It will now be proved that the Determinant Method may be applied to the operations table of equation (A8).

It is well-known (see reference 15) that any quadratic form Q may be put in the form

$$Q = \sum_{i=1}^{n} b_i (L_i)^2 \tag{A9}$$

where the b_i quantities are constants, and

$$L_i = \sum_{j=1}^{n} c_j x_j \tag{A10}$$

where the c_j quantities are constants. It is assumed that there are n linearly independent quantities L_i. This assumption entails no loss of generality since in the case in which it is not true some of the constants b_i will be zero.

By means of equation (A9) and table 2 of reference 2 the following table may be set up:

Sign of b_i	Sign of Q	Classification of Q	Type of equilibrium
All, less than zero	$Q < 0$ always ($Q = 0$ if $x_j \equiv 0$)	Negative definite nonsingular	Stable
Varying; none, zero	Q may be positive, negative, or zero	Indefinite nonsingular	Unstable
All, greater than zero	$Q > 0$ always ($Q = 0$ if $x_j \equiv 0$)	Positive definite nonsingular	Unstable
Some, zero; all others, negative	$Q = 0$ or $Q < 0$	Negative definite singular	Neutral
Some, zero; others, varying	Q may be positive, negative, or zero	Indefinite singular	Unstable
Some, zero; all others, positive	$Q = 0$ or $Q > 0$	Positive definite singular	Unstable

Two conditions for neutral equilibrium have been thus set up:

(1) The vanishing of the determinant A_n of the quadratic form Q

(2) The fact that some of the b_i's equal zero, while all others are negative

As both conditions are necessary and sufficient, they are equivalent and may be used interchangeably.

When some of the displacements are guessed as previously explained, the quadratic form Q becomes the reduced quadratic form Q', where

$$Q' = \sum_{i=1}^{p} b_i' \left(L_i'\right)^2 \tag{A11}$$

where the b_i' quantities are constants and

$$L_i' = c_p' + \sum_{j=1}^{p-1} c_j' x_j \tag{A12}$$

The statements of the above table may now be applied to the quadratic form Q', since Q' is the value the quadratic form Q will take on when the displacements $x_p, \ldots, x_n$ are assumed. Neutral equilibrium will then exist when some of the b_i's are zero and all others are negative. But this condition is equivalent to the condition that the determinant corresponding to the quadratic form Q' must vanish. This determinant is obtained by multiplying out the right-hand side of equation (A11) and expressing the result in the form

$$Q' = \sum_{i=1}^{p-1} \sum_{j=1}^{p-1} a_{ij} x_i x_j + \sum_{i=1}^{p-1} a'_{ip} x_i + \sum_{j=1}^{p-1} a'_{pi} x_i + a'_{pp} \tag{A13}$$

The determinant corresponding to Q' will then be seen to be identical with A' of equation (A8).

It therefore follows that the vanishing of the determinant A' of equation (A8) corresponds to neutral equilibrium. If the displacements $x_p, \ldots, x_n$ were not chosen exactly equal to the displacements of the structure at buckling, an approximate value of the buckling load will be obtained rather than an exact one. It was proved in reference 2 that this approximate load will be higher than the actual one.

APPENDIX B

GENERAL FORMULAS AND NUMERICAL EXAMPLE

In this appendix is presented the procedure for the determination of the influence coefficients required in setting up the operations tables II and III. Since many of the formulas used in the analysis are scattered throughout the literature, some of these are given here, together with appropriate reference. When a formula is not listed, reference to its source is given. A numerical example is also given illustrating both methods suggested for the calculation of the buckling loads of cylinders without cutout.

Influence Coefficients

The operations tables (tables II and III) contain three types of influence coefficients, which represent the effects of the rings, the sheet covering, and the stringers. The methods by which each type is determined are outlined below.

Ring influence coefficients.- The ring influence coefficients are characterized by the symbol $\frown$, as, for example, $\widehat{rr}_M$, $\widehat{rt}_M$, or $\widehat{tn}_F$. These coefficients may be determined from reference 11, in which they may be seen to depend on the three parameters β, γ, and ξ, where β is the central angle of the ring segment, and γ and ξ are defined in equations (7). Any one of the three following ways may be used for the calculation of these coefficients:

(1) General formulas are given in equations (20), (27), (28), and (29) of reference 11. As an example, the formula for rt_M is repeated here with a slight change in notation:

$$-\widehat{rt}_M \frac{d^3}{(EI)_r} = -\widehat{tr}_M \frac{d^3}{(EI)_r} = \beta^3 \frac{\Delta\widehat{tr}}{\Delta} \frac{r^3}{(EI)_r} \tag{B1}$$

where

$$-\Delta_{tr} \frac{r}{\beta^4 (EI)_r} = f_{tr1} + (1/\gamma)\left[(1/\xi) - 1\right] f_{tr2}$$

and

$$\frac{\Delta}{r^2\beta^7} = f_{\Delta 1} + (1/\gamma)\left[f_{\Delta 2} + (1/\xi)(f_{\Delta 3})\right] + (1/\gamma)^2\left\{(1/\xi) + \left[(1/\xi) - 1\right]^2 f_{\Delta 4}\right\}$$

in which the quantities f are functions of the central angle β and are given in reference 11 by equations (24) and, for specific values of β, by table II and figures 3 to 13.

(2) Influence coefficients obtained from the formulas mentioned under item (1) are tabulated in tables III and IV of reference 11 for specific values of the parameters β, γ, and ξ.

(3) From the tabulated values mentioned in item (2) above, curves were plotted which are presented in figures 14 to 85 of reference 11. It should be noted that in general these curves are accurate only for values of $\beta \geq 15^\circ$.

Sheet influence coefficients.- The shear in the sheet covering is represented by the influence coefficients containing the quantities α and Λ_I, as, for example, $2\alpha_r{}^2\Lambda_I$ or $2\alpha_t\alpha_n\Lambda_I\, d_I$. The quantities α may be determined in good approximation from the formulas

$$\left.\begin{aligned} \alpha_r &= 0.1\beta \\ \alpha_t &= -0.5(1 - 0.01666 \cdot \cdot \cdot \beta^2) \\ \alpha_n &= -0.008333 \cdot \cdot \cdot \beta(1 + 0.014286\beta^2) \end{aligned}\right\} \qquad \text{(B2)}$$

taken from page 27 of reference 11. It should be noted that in this reference α_r, α_t, and α_n are denoted as $r_q/(Lq)$, $t_q/(Lq)$, and $n_q/(L^2q)$, respectively.

The quantity Λ_I is given by

$$\Lambda_I = G_{eff}\frac{td_I}{L} \qquad \text{(B3)}$$

where the effective shear modulus G_{eff} is given by equation (8) of the present report.

The buckling strain ϵ_{cr} of a sheet panel appearing in this equation was obtained by means of Redshaw's formula:

$$\epsilon_{cr} = \left(\epsilon_{flat}/2\right) + \sqrt{\left(\epsilon_{flat}/2\right)^2 + \left(\epsilon_{curved}\right)^2} \tag{B4}$$

where

$$\epsilon_{flat} = \frac{k'\pi^2}{12\left(1 - \nu^2\right)}\left(\frac{t}{d}\right)^2 \tag{B5}$$

as shown in reference 16, in which k' is the end-fixity coefficient, ν is Poisson's ratio, and

$$\epsilon_{curved} = 0.6(t/r)\,\frac{1 - 1.7 \times 10^{-7}(r/t)^2}{1 + 0.004\left(E/F_{cy}\right)} \tag{B6}$$

as shown in reference 17, in which F_{cy} is the yield stress of the material.

The effect of normal stresses in the sheet covering is taken into account by an effective width of sheet as discussed in the next section.

Stringer beam-column influence coefficients.- The beam-column effects in the stringers are represented by the influence coefficients containing the load P, as, for example, $\left(P/D_1\right)(1 - c)$ or Pks/D_1. A complete list of beam-column influence coefficients is presented in tables VI, VII, and VIII in which the sign convention as well as definitions of symbols are given. All these coefficients are functions of the quantity k defined in equation (2). The following formula which was derived in reference 18 on the basis of work contained in reference 19 is suggested for the calculation of the effective width $2w$:

$$2w = (1/\epsilon)(d/r)\left\{0.3t + 1.535\left[(t/d)(r\epsilon - 0.3t)r^{1/2}\right]^{2/3}\right\} \tag{B7}$$

If the load P causes a stringer stress which is higher than the proportional limit of the material, the modulus of elasticity E which

appears in equation (2) must be reduced in an appropriate manner. In this investigation Von Kármán's formula was used:

$$E_{red} = 4\,EE_t \Big/ \left(\sqrt{E} + \sqrt{E_t}\right)^2 \tag{B8}$$

where E_t is the tangent modulus.

Numerical Example

As an example of the application of the methods suggested for the calculation of the buckling load of cylinders without cutout the buckling load is determined here for GALCIT cylinder 65 of reference 8. The characteristics of this cylinder are given in figure 1. Table I is readily set up with the aid of these characteristics and the equations listed in the previous section. The influence coefficients required for tables II or III can then be calculated.

Ring influence coefficients.- The values of the ring influence coefficients corresponding to β_I, γ_I, and ξ_I (see table I) happen to appear in tables III of reference 11. However, since these tables do not contain coefficients corresponding to ξ_{II}, it is necessary to use values interpolated from the appropriate curves of reference 11. The following values were obtained for the ring influence coefficients:

Ring segment I	Ring segment II
$\widehat{nn}_{M_I}\left(\frac{d_I}{EI_r}\right) = 6.393$	$\widehat{nn}_{M_{II}}\left(\frac{d_{II}}{EI_r}\right) = 8.65$
$\widehat{rn}_{M_I}\left(\frac{d_I^2}{EI_r}\right) = -20.38$	$\widehat{rn}_{M_{II}}\left(\frac{d_{II}^2}{EI_r}\right) = -33.0$
$\widehat{tn}_{M_I}\left(\frac{d_I^2}{EI_r}\right) = 109.0$	$\widehat{tn}_{M_{II}}\left(\frac{d_{II}^2}{EI_r}\right) = 33.0$
$\widehat{rr}_{M_I}\left(\frac{d_I^3}{EI_r}\right) = 98.43$	$\widehat{rr}_{M_{II}}\left(\frac{d_{II}^3}{EI_r}\right) = 170$

$$\widehat{tr}_{M_I}\left(\frac{d_I^3}{EI_r}\right) = -656.6 \qquad \widehat{tr}_{M_{II}}\left(\frac{d_{II}^3}{EI_r}\right) = -200$$

$$\widehat{tt}_{M_I}\left(\frac{d_I^3}{EI_r}\right) = 4999 \qquad \widehat{tt}_{M_{II}}\left(\frac{d_{II}^3}{EI_r}\right) = 280$$

$$\widehat{rn}_{F_I}\left(\frac{d_I^2}{EI_r}\right) = -8.531$$

$$\widehat{rr}_{F_I}\left(\frac{d_I^3}{EI_r}\right) = 74.86$$

$$\widehat{tr}_{F_I}\left(\frac{d_I^3}{EI_r}\right) = -659.7$$

Sheet influence coefficients.- The quantities α of equation (B2) have the following values:

Bay I	Bay II
$\alpha_r = 0.0261$	No sheet in this bay
$\alpha_t = -0.499$	
$\alpha_n = -0.00218$	

Stringer beam-column influence coefficients.- For an assumed load P = 1550 pounds a typical set of calculated results is given below (see tables I and VI and equations (2) and (B8)).

P (lb)	σ (psi)	E_{red} (psi)	$E_{red} I_{str_r}$	k	kL	sin kL	cos kL
1550	37,300	7.056×10^6	4000	0.6225	2.490	0.60646	-0.79511

The beam-column influence coefficients required for table II are then

$$\frac{Pks}{D_1} = 281.31 \qquad \frac{P(kL - s)}{kD_1} = 2254.6$$

$$\frac{P(1 - c)}{D_1} = 1337.6 \qquad \frac{2P}{kD_1}(s - kLc) = 6191.7$$

No beam-column influence coefficients need be calculated if table III and figure 3 are used.

Calculation of buckling load by table II.- The state of stability of the structure at a load of $P = 1550$ pounds may now be investigated by introducing all the above influence coefficients into table II and evaluating the corresponding determinant. The results corresponding to the assumed load of 1550 pounds, as well as those for the loads of 1650, 1680, and 1715 pounds, are presented in figure 5. In this figure are plotted both the values of the determinant and the values of the last main-diagonal term a_{nn} of the auxiliary matrix of reference 3. The intercept of the curves in this figure may be read off and corresponds to the buckling load. It should be noted that only the stringer beam-column influence coefficients vary as the assumed load is changed.

Calculation of buckling load by table III.- The value of the quantity K of equation (3) was found by the method of reference 3 to be -5.472. From figure 3, this value may be seen to correspond to $kL = 3.4$, from which $P_{cr} = 1730$ pounds. Care must be taken that a reduced modulus (equation (B8)) be used if the stress at buckling is above the proportional limit.

APPENDIX C

SYMBOLS

$A_1, A_2, \cdots A_i, \cdots A_n$	determinants or matrices
$A_{eff_{str}}$	effective cross-sectional area of stringer
A_r	effective cross-sectional area of ring
$A_r{}^*$	effective shear area of ring cross section
A'	reduced matrix
A, B, C, D	rings
E	Young's modulus
$(EI)_r$	bending rigidity of a ring in its own plane
$(EI)_{str_r}$	radial bending rigidity of stringer and its effective width of sheet
E_{red}	reduced modulus
E_t	tangent modulus
F_{cy}	yield-point stress
F_i	generalized external force
G_{eff}	effective shear modulus
$G_{eff_{red}}$	reduced effective shear modulus
G_0	shear modulus of sheet material under no compressive load
I_r	moment of inertia of ring cross section plus effective width

I_{str_r} moment of inertia of stringer plus effective width of sheet for radial bending

K constant

L ring spacing

L_i linear function

L'/D ratio of total cylinder length to cylinder diameter

M_t moment causing bending of stringer (vector pointing in tangential direction)

N moment causing bending of ring in its plane; also $0.0275\ [(2\pi r/d) + 1]$

P axial stringer load

P_{cr} load in the most highly compressed stringer at the instant of buckling

Q quadratic form

Q' reduced quadratic form

R radial force

T tangential force

a_{ij} element of operations table

a'_{ip} element of last row or column of reduced matrix

b_i, b_i' constants

c_j, c_j' constants

d circumferential stringer spacing

f function of β

f(kL) function of kL

i, j indices

$k = \sqrt{P/(EI)_{str_r}}$

k'	end-fixity coefficient
m_t	rotation causing bending of stringer (vector pointing in tangential direction)
n	number of stringers; number of generalized displacements; rotation causing bending of ring in its plane
p	index
r	radius; radial displacement
$\widehat{rr}$, $\widehat{rm}$, $\widehat{rt}$, and so forth	ring influence coefficients
t	sheet thickness; tangential displacement
$2w$	effective width of sheet
x	longitudinal axis of stringer
x_j	generalized displacement
Γ	parameter
Λ	parameter
Λ_I	parameter $\left(\frac{G_{eff}td_I}{L}\right)$
α_{ij}	auxiliary-matrix element
α_{nn}	last main-diagonal element of auxiliary matrix
α_r, α_t, α_n	functions of β required for sheet influence coefficients
β	central angle of a ring segment (d/r)
γ	parameter; shear strain
ϵ	strain in most highly compressed stringer at failure
ϵ_{cr}	buckling strain of a sheet panel
ϵ_{curved}	buckling strain of nonreinforced circular cylinder under uniform axial compression

ϵ_{flat}	buckling strain of flat panel under uniform compression
ν	Poisson's ratio
ξ	parameter
σ	compressive stringer stress
τ	shear stress

Subscripts:

A, B, C, D	rings
F	fixed
M	movable
av	average
exp	experiment
1, 2, 3	stringers
I, II	regions

REFERENCES

1. Southwell, R. V.: Relaxation Methods in Engineering Science. A Treatise on Approximate Computations. The Clarendon Press (Oxford), 1940.

2. Boley, Bruno A.: Numerical Methods for the Calculation of Elastic Instability. Jour. Aero. Sci., vol. 14, no. 6, June 1947, pp. 337-348.

3. Crout, Prescott D.: A Short Method for Evaluating Determinants and Solving Systems of Linear Equations with Real or Complex Coefficients. Trans. AIEE, vol. 60, 1941, pp. 1235-1240.

4. Hoff, N. J., Levy, Robert S., and Kempner, Joseph: Numerical Procedures for the Calculation of the Stresses in Monocoques. I - Diffusion of Tensile Stringer Loads in Reinforced Panels. NACA TN 934, 1944.

5. Hoff, N. J., and Boley, Bruno A.: The Shear Rigidity of Curved Panels under Compression. NACA TN 1090, 1946.

6. GALCIT: Some Investigations of the General Instability of Stiffened Metal Cylinders. IV - Continuation of Tests of Sheet-Covered Specimens and Studies of the Buckling Phenomena of Unstiffened Circular Cylinders. NACA TN 908, 1943.

7. GALCIT: Some Investigations of the General Instability of Stiffened Metal Cylinders. VI - Stiffened Metal Cylinders Subjected to Combined Bending and Transverse Shear. NACA TN 910, 1943.

8. GALCIT: Some Investigations of the General Instability of Stiffened Metal Cylinders. V - Stiffened Metal Cylinders Subjected to Pure Bending. NACA TN 909, 1943.

9. Hoff, N. J., Fuchs, S. J., and Cirillo, Adam J.: The Inward Bulge Type Buckling of Monocoque Cylinders. II - Experimental Investigation of the Buckling in Combined Bending and Compression. NACA TN 939, 1944.

10. Hoff, N. J., Klein, Bertram, and Boley, Bruno A.: The Inward Bulge Type Buckling of Monocoque Cylinders. V - Revised Strain Energy Theory Which Assumes a More General Deflected Shape. NACA TN 1505, 1948.

11. Hoff, N. J., Klein, Bertram, and Libby, Paul A.: Numerical Procedures for the Calculation of the Stresses in Monocoques. IV - Influence Coefficients of Curved Bars for Distortions in Their Own Plane. NACA TN 999, 1946.

12. Hoff, N. J.: General Instability of Monocoque Cylinders. Jour. Aero. Sci., vol. 10, no. 4, April 1943, pp. 105-114, 130.

13. Hoff, N. J., Boley, Bruno A., and Nardo, S. V.: The Inward Bulge Type Buckling of Monocoque Cylinders. IV - Experimental Investigation of Cylinders Subjected to Pure Bending. NACA TN 1499, 1948.

14. Kromm, A., and Marguerre, K.: Behavior of a Plate Strip under Shear and Compressive Stresses beyond the Buckling Limit. NACA TM 870, 1938.

15. Bôcher, Maxime: Introduction to Higher Algebra. The Macmillan Co., 1931.

16. Timoshenko, S.: Theory of Plates and Shells. First Ed., McGraw-Hill Book Co., Inc., 1940.

17. Donnell, L. H.: A New Theory for the Buckling of Thin Cylinders under Axial Compression and Bending. Trans. A.S.M.E., vol. 56, no. 11, Nov. 1934, pp. 795-806.

18. Hoff, N. J., and Klein, Bertram: The Inward Bulge Type Buckling of Monocoque Cylinders. I - Calculation of the Effect upon the Buckling Stress of a Compressive Force, a Nonlinear Direct Stress Distribution, and a Shear Force. NACA TN 938, 1944.

19. Ebner, H.: The Strength of Shell Bodies - Theory and Practice. NACA TM 838, 1937.

20. Templin, R. L., Hartmann, E. C., and Paul, D. A.: Typical Tensile and Compressive Stress-Strain Curves for Aluminum Alloy 24S-T, Alclad 24S-T, 24S-RT, and Alclad 24S-RT Products. Tech. Paper No. 6, Aluminum Res. Lab., Aluminum Co. of Am., 1942.

TABLE I

CHARACTERISTICS OF CYLINDERS

Cylinder (1)	r (in.)	t (in.)	d_I (in.)	d_{II} (in.)	β_I (deg)	β_{II} (deg)	L (in.)	n
GALCIT 65	10	0.010	2.61	13.05	15	75	4	24
GALCIT 25	15.92	0.010	2.53	22.77	9	81	8	40
PIBAL 10	10	0.012	3.93	11.79	$22\frac{1}{2}$	$67\frac{1}{2}$	5	16

Cylinder	k'	ϵ_{flat}	ϵ_{curved}	ϵ_{cr}	ϵ (2)	2w (in.)	$A_{eff_{str}}$ (sq in.)	I_{str_r} $(in.^4)$	I_r $(in.^4)$	G_{eff} (psi)	γ_I	γ_{II}	ξ	Λ_I (lb/in.)
GALCIT 65	5.5	0.730×10^{-4}	2.430×10^{-4}	2.82×10^{-4}	31.5×10^{-4}	0.875	0.0415	5.669×10^{-4}	0.2194×10^{-4}	2.68×10^6	10,180	255,000	0.25	17,500
GALCIT 25	6	0.847	1.050	1.56	17.0	1.031	0.0429	5.898	0.2194	3.90	9,568	775,000	0.25	12,334
PIBAL 10	(3)	0.50	3.0	3.26	22.4	1.547	0.1596	22.40	0.8034	1.93	9,862	88,760	0.32	18,190

[1]All cylinders are aluminum ($E = 10.5 \times 10^6$ psi, $G_0 = 3.9 \times 10^6$ psi, $\nu = 0.3$, E_t from reference 20).

[2]In general ϵ must be guessed. In the present investigation ϵ was available from experimental results (references 8 and 9).

[3]k' not required since ϵ_{flat} and ϵ_{curved} are given in reference 9.

TABLE II

OPERATIONS TABLE FOR THE SIMPLIFIED STRUCTURE

	(1) r_{D2}	(2) r_{B2}	(3) t_{D2}	(4) n_{B2}	(5) t_{B2}	(6) n_{D2}	(7) r_{C2}	(8) t_{C2}	(9) n_{C2}	(10) $m_{t_{B1}}$	(11) $m_{t_{C1}}$	(12) r_{B1}	(13) r_{C1}	(14) r_{D1}
(1) R_{D2}	$-\hat{f}\hat{r}_{M_I}$ $-\hat{f}\hat{r}_{M_{II}}$ $-2\alpha_r^2\Lambda_1$	0	$\hat{f}\hat{t}_{M_I}$ $-\hat{f}\hat{t}_{M_{II}}$ $+2\alpha_r\alpha_t\Lambda_1$	0	0	$\hat{f}\hat{n}_{M_I}$ $-\hat{f}\hat{n}_{M_{II}}$ $+2\alpha_r\alpha_n\Lambda_1 d_1$	$2\alpha_r^2\Lambda_1$	$-2\alpha_r\alpha_t\Lambda_1$	$-2\alpha_r\alpha_n\Lambda_1 d_1$	0	0	0	$-2\alpha_r^2\Lambda_1$	$-\hat{f}\hat{r}_{F_I}$ $+2\alpha_r^2\Lambda_1$
(2) $2R_{B2}$	0	$-2\hat{f}\hat{r}_{M_I}$ $-2\hat{f}\hat{r}_{M_{II}}$ $-4\alpha_r^2\Lambda_1$	0	$2\hat{f}\hat{n}_{M_I}$ $-2\hat{f}\hat{n}_{M_{II}}$ $+4\alpha_r\alpha_n\Lambda_1 d_1$	$2\hat{f}\hat{t}_{M_I}$ $-2\hat{f}\hat{t}_{M_{II}}$ $+4\alpha_r\alpha_t\Lambda_1$	0	$2\alpha_r^2\Lambda_1$	$-2\alpha_r\alpha_t\Lambda_1$	$-2\alpha_r\alpha_n\Lambda_1 d_1$	0	0	$-2\hat{f}\hat{r}_{F_I}$ $+4\alpha_r^2\Lambda_1$	$-2\alpha_r^2\Lambda_1$	0
(3) T_{D2}	$\hat{f}\hat{r}_{M_I}$ $-\hat{f}\hat{r}_{M_{II}}$ $+2\alpha_t\alpha_r\Lambda_1$	0	$-\hat{f}\hat{t}_{M_I}$ $-\hat{f}\hat{t}_{M_{II}}$ $-2\alpha_t^2\Lambda_1$	0	0	$-\hat{f}\hat{n}_{M_I}$ $-\hat{f}\hat{n}_{M_{II}}$ $-2\alpha_t\alpha_n\Lambda_1 d_1$	$-2\alpha_t\alpha_r\Lambda_1$	$2\alpha_t^2\Lambda_1$	$2\alpha_t\alpha_n\Lambda_1 d_1$	0	0	0	$2\alpha_t\alpha_r\Lambda_1$	$\hat{f}\hat{r}_{F_I}$ $-2\alpha_t\alpha_r\Lambda_1$
(4) $2N_{B2}$	0	$2\hat{n}\hat{r}_{M_I}$ $-2\hat{n}\hat{r}_{M_{II}}$ $+4\alpha_n\alpha_r\Lambda_1 d_1$	0	$-2\hat{n}\hat{n}_{M_I}$ $-2\hat{n}\hat{n}_{M_{II}}$ $-4\alpha_n^2\Lambda_1 d_1^2$	$-2\hat{n}\hat{t}_{M_I}$ $-2\hat{n}\hat{t}_{M_{II}}$ $-4\alpha_n\alpha_t\Lambda_1 d_1$	0	$-2\alpha_n\alpha_r\Lambda_1 d_1$	$2\alpha_n\alpha_t\Lambda_1 d_1$	$2\alpha_n^2\Lambda_1^2 d_1^2$	0	0	$2\hat{n}\hat{r}_{F_I}$ $-4\alpha_n\alpha_r\Lambda_1 d_1$	$2\alpha_n\alpha_r\Lambda_1 d_1$	0
(5) $2T_{B2}$	0	$2\hat{t}\hat{r}_{M_I}$ $-2\hat{t}\hat{r}_{M_{II}}$ $+4\alpha_t\alpha_r\Lambda_1$	0	$-2\hat{t}\hat{n}_{M_I}$ $-2\hat{t}\hat{n}_{M_{II}}$ $-4\alpha_t\alpha_n\Lambda_1 d_1$	$-2\hat{t}\hat{t}_{M_I}$ $-2\hat{t}\hat{t}_{M_{II}}$ $-4\alpha_t^2\Lambda_1$	0	$-2\alpha_t\alpha_r\Lambda_1$	$2\alpha_t^2\Lambda_1$	$2\alpha_t\alpha_n\Lambda_1 d_1$	0	0	$2\hat{t}\hat{r}_{F_I}$ $-4\alpha_t\alpha_r\Lambda_1$	$2\alpha_t\alpha_r\Lambda_1$	0
(6) N_{D2}	$\hat{n}\hat{r}_{M_I}$ $-\hat{n}\hat{r}_{M_{II}}$ $+2\alpha_n\alpha_r\Lambda_1 d_1$	0	$-\hat{n}\hat{t}_{M_I}$ $-\hat{n}\hat{t}_{M_{II}}$ $-2\alpha_n\alpha_t\Lambda_1 d_1$	0	0	$-\hat{n}\hat{n}_{M_I}$ $-\hat{n}\hat{n}_{M_{II}}$ $-2\alpha_n^2\Lambda_1 d_1^2$	$-2\alpha_n\alpha_r\Lambda_1 d_1$	$2\alpha_n\alpha_t\Lambda_1 d_1$	$2\alpha_n^2\Lambda_1^2 d_1^2$	0	0	0	$2\alpha_n\alpha_r\Lambda_1 d_1$	$\hat{n}\hat{r}_{F_I}$ $-2\alpha_n\alpha_r\Lambda_1 d_1$
(7) $2R_{C2}$	$2\alpha_r^2\Lambda_1$	$2\alpha_r^2\Lambda_1$	$-2\alpha_r\alpha_t\Lambda_1$	$-2\alpha_r\alpha_n\Lambda_1 d_1$	$-2\alpha_r\alpha_t\Lambda_1$	$-2\alpha_r\alpha_n\Lambda_1 d_1$	$-2\hat{f}\hat{r}_{M_I}$ $-2\hat{f}\hat{r}_{M_{II}}$ $-4\alpha_r^2\Lambda_1$	$2\hat{f}\hat{t}_{M_I}$ $-2\hat{f}\hat{t}_{M_{II}}$ $+4\alpha_r\alpha_t\Lambda_1$	$2\hat{f}\hat{n}_{M_I}$ $-2\hat{f}\hat{n}_{M_{II}}$ $+4\alpha_r\alpha_n\Lambda_1 d_1$	0	0	$-2\alpha_r^2\Lambda_1$	$-2\hat{f}\hat{r}_{F_I}$ $+4\alpha_r^2\Lambda_1$	$-2\alpha_r^2\Lambda_1$
(8) $2T_{C2}$	$-2\alpha_t\alpha_r\Lambda_1$	$-2\alpha_t\alpha_r\Lambda_1$	$2\alpha_t^2\Lambda_1$	$2\alpha_t\alpha_n\Lambda_1 d_1$	$2\alpha_t^2\Lambda_1$	$2\alpha_t\alpha_n\Lambda_1 d_1$	$2\hat{f}\hat{r}_{M_I}$ $-2\hat{f}\hat{r}_{M_{II}}$ $+4\alpha_t\alpha_r\Lambda_1$	$-2\hat{f}\hat{t}_{M_I}$ $-2\hat{f}\hat{t}_{M_{II}}$ $-4\alpha_t^2\Lambda_1$	$-2\hat{f}\hat{n}_{M_I}$ $-2\hat{f}\hat{n}_{M_{II}}$ $-4\alpha_t\alpha_n\Lambda_1 d_1$	0	0	$2\alpha_t\alpha_r\Lambda_1$	$2\hat{f}\hat{r}_{F_I}$ $-4\alpha_t\alpha_r\Lambda_1$	$2\alpha_t\alpha_r\Lambda_1$
(9) $2N_{C2}$	$-2\alpha_n\alpha_r\Lambda_1 d_1$	$-2\alpha_n\alpha_r\Lambda_1 d_1$	$2\alpha_n\alpha_t\Lambda_1 d_1$	$2\alpha_n^2\Lambda_1 d_1^2$	$2\alpha_n\alpha_t\Lambda_1 d_1$	$2\alpha_n^2\Lambda_1 d_1^2$	$2\hat{n}\hat{r}_{M_I}$ $-2\hat{n}\hat{r}_{M_{II}}$ $+4\alpha_n\alpha_r\Lambda_1 d_1$	$-2\hat{n}\hat{t}_{M_I}$ $-2\hat{n}\hat{t}_{M_{II}}$ $-4\alpha_n\alpha_t\Lambda_1 d_1$	$-2\hat{n}\hat{n}_{M_I}$ $-2\hat{n}\hat{n}_{M_{II}}$ $-4\alpha_n^2\Lambda_1 d_1^2$	0	0	$2\alpha_n\alpha_r\Lambda_1 d_1$	$2\hat{n}\hat{r}_{F_I}$ $-4\alpha_n\alpha_r\Lambda_1 d_1$	$2\alpha_n\alpha_r\Lambda_1 d_1$
(10) $M_{t_{B1}}$	0	0	0	0	0	0	0	0	0	$-\frac{2P}{kD_1}(s-kL_c)$	$-\frac{P}{kD_1}(kL-s)$	0	$\frac{P}{D_1}(1-c)$	0
(11) $M_{t_{C1}}$	0	0	0	0	0	0	0	0	0	$-\frac{P}{kD_1}(kL-s)$	$-\frac{2P}{kD_1}(s-kL_c)$	$-\frac{P}{D_1}(1-c)$	0	$\frac{P}{D_1}(1-c)$
(12) R_{B1}	0	$-2\hat{f}\hat{r}_{F_I}$ $+4\alpha_r^2\Lambda_1$	0	$2\hat{f}\hat{n}_{F_I}$ $-4\alpha_r\alpha_n\Lambda_1 d_1$	$2\hat{f}\hat{t}_{F_I}$ $-4\alpha_r\alpha_t\Lambda_1$	0	$-2\alpha_r^2\Lambda_1$	$2\alpha_r\alpha_t\Lambda_1$	$2\alpha_r\alpha_n\Lambda_1 d_1$	0	$-\frac{P}{D_1}(1-c)$	$-2\hat{f}\hat{r}_{M_I}$ $-4\alpha_r^2\Lambda_1$ $-2Pks/D_1$	$2\alpha_r^2\Lambda_1$ $+Pks/D_1$	0
(13) R_{C1}	$-2\alpha_r^2\Lambda_1$	$-2\alpha_r^2\Lambda_1$	$2\alpha_r\alpha_t\Lambda_1$	$2\alpha_r\alpha_n\Lambda_1 d_1$	$2\alpha_r\alpha_t\Lambda_1$	$2\alpha_r\alpha_n\Lambda_1 d_1$	$-2\hat{f}\hat{r}_{F_I}$ $+4\alpha_r^2\Lambda_1$	$2\hat{f}\hat{t}_{F_I}$ $-4\alpha_r\alpha_t\Lambda_1$	$2\hat{f}\hat{n}_{F_I}$ $-4\alpha_r\alpha_n\Lambda_1 d_1$	$\frac{P}{D_1}(1-c)$	0	$2\alpha_r^2\Lambda_1$ $+Pks/D_1$	$-2\hat{f}\hat{r}_{M_I}$ $-4\alpha_r^2\Lambda_1$ $-2Pks/D_1$	$2\alpha_r^2\Lambda_1$ $+Pks/D_1$
(14) $R_{D1}/2$	$-\hat{f}\hat{r}_{F_I}$ $+2\alpha_r^2\Lambda_1$	0	$\hat{f}\hat{t}_{F_I}$ $-2\alpha_r\alpha_t\Lambda_1$	0	0	$\hat{f}\hat{n}_{F_I}$ $-2\alpha_r\alpha_n\Lambda_1 d_1$	$-2\alpha_r^2\Lambda_1$	$2\alpha_r\alpha_t\Lambda_1$	$2\alpha_r\alpha_n\Lambda_1 d_1$	0	$\frac{P}{D_1}(1-c)$	0	$2\alpha_r^2\Lambda_1$ $+Pks/D_1$	$-\hat{f}\hat{r}_{M_I}$ $-2\alpha_r^2\Lambda_1$ $-Pks/D_1$

NACA

TABLE III

OPERATIONS TABLE FOR SOLUTION WITH ASSUMED DISPLACEMENTS

	(1) r_{D2}	(2) r_{B2}	(3) t_{D2}	(4) n_{B2}	(5) t_{B2}	(6) n_{D2}	(7) r_{C2}	(8) t_{C2}	(9) n_{C2}	(10') 1
(1) R_{D2}	$-\hat{r}r_{M_I}$ $-\hat{r}r_{M_{II}}$ $-2\alpha_r^2\Lambda_I$	0	$\hat{r}t_{M_I}$ $-\hat{r}t_{M_{II}}$ $+2\alpha_r\alpha_t\Lambda_I$	0	0	$\hat{r}n_{M_I}$ $-\hat{r}n_{M_{II}}$ $+2\alpha_r\alpha_n\Lambda_I d_I$	$2\alpha_r^2\Lambda_I$	$-2\alpha_r\alpha_t\Lambda_I$	$-2\alpha_r\alpha_n\Lambda_I d_I$	$1.0257\alpha_r^2\Lambda_I-\hat{r}r_{F_I}$
(2) $2R_{B2}$		$-2\hat{r}r_{M_I}$ $-2\hat{r}r_{M_{II}}$ $-4\alpha_r^2\Lambda_I$	0	$2\hat{r}n_{M_I}$ $-2\hat{r}n_{M_{II}}$ $+4\alpha_r\alpha_n\Lambda_I d_I$	$2\hat{r}t_{M_I}$ $-2\hat{r}t_{M_{II}}$ $+4\alpha_r\alpha_t\Lambda_I$	0	$2\alpha_r^2\Lambda_I$	$-2\alpha_r\alpha_t\Lambda_I$	$-2\alpha_r\alpha_n\Lambda_I d_I$	$-0.84926\alpha_r^2\Lambda_I-0.06250\hat{r}r_{F_I}$
(3) T_{D2}			$-\hat{t}t_{M_I}$ $-\hat{t}t_{M_{II}}$ $-2\alpha_t^2\Lambda_I$	0	0	$-\hat{t}n_{M_I}$ $-\hat{t}n_{M_{II}}$ $-2\alpha_t\alpha_n\Lambda_I d_I$	$-2\alpha_t\alpha_r\Lambda_I$	$2\alpha_t^2\Lambda_I$	$2\alpha_t\alpha_n\Lambda_I d_I$	$-1.0257\alpha_t\alpha_r\Lambda_I+\hat{t}r_{F_I}$
(4) $2N_{B2}$				$-2\hat{n}n_{M_I}$ $-2\hat{n}n_{M_{II}}$ $-4\alpha_n^2\Lambda_I d_I^2$	$-2\hat{n}t_{M_I}$ $-2\hat{n}t_{M_{II}}$ $-4\alpha_n\alpha_t\Lambda_I d_I$	0	$-2\alpha_n\alpha_r\Lambda_I d_I$	$2\alpha_n\alpha_t\Lambda_I d_I$	$2\alpha_n^2\Lambda_I d_I^2$	$0.84926\alpha_n\alpha_r\Lambda_I d_I+0.06250\hat{n}r_{F_I}$
(5) $2T_{B2}$					$-2\hat{t}t_{M_I}$ $-2\hat{t}t_{M_{II}}$ $-4\alpha_t^2\Lambda_I$	0	$-2\alpha_t\alpha_r\Lambda_I$	$2\alpha_t^2\Lambda_I$	$2\alpha_t\alpha_n\Lambda_I d_I$	$0.84926\alpha_t\alpha_r\Lambda_I+0.06250\hat{t}r_{F_I}$
(6) N_{D2}						$-\hat{n}n_{M_I}$ $-\hat{n}n_{M_{II}}$ $-2\alpha_n^2\Lambda_I d_I^2$	$-2\alpha_n\alpha_r\Lambda_I d_I$	$2\alpha_n\alpha_t\Lambda_I d_I$	$2\alpha_n^2\Lambda_I d_I^2$	$-1.0257\alpha_n\alpha_r\Lambda_I d_I+\hat{n}r_{F_I}$
(7) $2R_{C2}$							$-2\hat{r}r_{M_I}$ $-2\hat{r}r_{M_{II}}$ $-4\alpha_r^2\Lambda_I$	$2\hat{r}t_{M_I}$ $-2\hat{r}t_{M_{II}}$ $+4\alpha_r\alpha_t\Lambda_I$	$2\hat{r}n_{M_I}$ $-2\hat{r}n_{M_{II}}$ $+4\alpha_r\alpha_n\Lambda_I d_I$	$-0.11398\alpha_r^2\Lambda_I-0.97426\hat{r}r_{F_I}$
(8) $2T_{C2}$								$-2\hat{t}t_{M_I}$ $-2\hat{t}t_{M_{II}}$ $-4\alpha_t^2\Lambda_I$	$-2\hat{t}n_{M_I}$ $-2\hat{t}n_{M_{II}}$ $-4\alpha_t\alpha_n\Lambda_I d_I$	$0.11398\alpha_t\alpha_r\Lambda_I+0.97426\hat{t}r_{F_I}$
(9) $2N_{C2}$									$-2\hat{n}n_{M_I}$ $-2\hat{n}n_{M_{II}}$ $-4\alpha_n^2\Lambda_I d_I^2$	$0.11398\alpha_n\alpha_r\Lambda_I d_I+0.97426\hat{n}r_{F_I}$
(10') 1										$\frac{(EI)_{str_r}}{L^3}f(kL)-0.94370\alpha_r^2\Lambda_I-1.4765\hat{r}r_{M_I}$

$$f(kL)=\frac{(kL)^2}{D_I}\left(-0.91592\frac{\sin kL}{kL}-0.44020\cos kL-0.47180kL\sin kL+1.3561\right)$$

TABLE IV

COMPARISON OF CALCULATED AND EXPERIMENTAL BUCKLING LOADS

Cylinder	Method of calculation	Calculated P_{cr} (lb)	Experimental P_{cr} (lb)	Difference (percent)
GALCIT 25	Table II	955	769	24.2
GALCIT 65	Table II	1670	1371	21.8
GALCIT 65	Table III	1730	1371	26.2
PIBAL 10	Table II	4850	3754	29.2

TABLE V

ASSUMED, CALCULATED, AND EXPERIMENTAL DEFLECTED SHAPES

[For sign convention and nomenclature see fig. 2]

Shape	r_B	r_C	r_D	m_B	m_C
$\sin^4\left(\frac{\pi x}{6L}\right)$	0.06250	0.56250	1	0.22672(1/L)	0.68016(1/L)
$\sin^5\left(\frac{\pi x}{6L}\right)$	0.031250	0.48713	1	0.14170(1/L)	0.73636(1/L)
$\sin^6\left(\frac{\pi x}{6L}\right)$	0.015625	0.42188	1	0.085020(1/L)	0.76520(1/L)
PIBAL cyl. 10 (Calculated)	-0.016949	0.50229	1	0.15086(1/L)	0.80011(1/L)
GALCIT cyl. 25 (Calculated)	0.066323	0.48355	1	0.093608(1/L)	0.82808(1/L)
GALCIT cyl. 65 (Calculated)	-0.16089	0.30640	1	-0.21075(1/L)	1.1631(1/L)
GALCIT cyl. 25 (Experimental)	0.222	0.667	1	----------	----------
GALCIT cyl. 27 (Experimental)	0.0370	0.204	1	----------	----------
GALCIT cyl. 30 (Experimental)	0.0588	0.412	1	----------	----------
GALCIT cyl. 35 (Experimental)	0.0893	0.446	1	----------	----------

TABLE VI

BEAM-COLUMN INFLUENCE COEFFICIENTS

[Compression]

Displacement	Unit	Forces (1)			
		F_A	M_A	F_B	M_B
δ_A	Both ends fixed	$-P\frac{ks}{D_1}$	$-P\frac{1-c}{D_1}$	$P\frac{ks}{D_1}$	$-P\frac{1-c}{D_1}$
m_A		$-P\frac{1-c}{D_1}$	$-\frac{P}{k}\frac{s-kLc}{D_1}$	$P\frac{1-c}{D_1}$	$-\frac{P}{k}\frac{Lk-s}{D_1}$
δ_B		$P\frac{ks}{D_1}$	$P\frac{1-c}{D_1}$	$-P\frac{ks}{D_1}$	$P\frac{1-c}{D_1}$
m_B		$-P\frac{1-c}{D_1}$	$-\frac{P}{k}\frac{Lk-s}{D_1}$	$P\frac{1-c}{D_1}$	$-\frac{P}{k}\frac{s-kLc}{D_1}$
δ_A	End A fixed	$-P\frac{k}{tD_2}$	$-P\frac{1}{D_2}$	$P\frac{k}{tD_2}$	0
m_A	End B pin-jointed	$-P\frac{1}{D_2}$	$-P\frac{L}{D_2}$	$P\frac{1}{D_2}$	0
δ_B		$P\frac{k}{tD_2}$	$P\frac{1}{D_2}$	$-P\frac{k}{tD_2}$	0
δ_A	Both ends pin-jointed	$\frac{P}{L}$	0	$-\frac{P}{L}$	0
δ_B		$-\frac{P}{L}$	0	$\frac{P}{L}$	0

[1] $D_1 = 2(1 - c) - kLs$
$D_2 = 1 - (kL/t)$
$k^2 = P/EI$

$s = \sin kL$
$c = \cos kL$
$t = \tan kL$

Sign convention
Forces on constraints

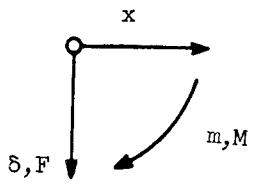

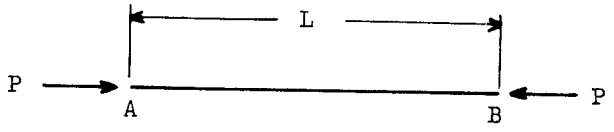

P, positive as shown

TABLE VII

BEAM-COLUMN INFLUENCE COEFFICIENTS

[Axial end load P equal to zero]

Displacement	Unit	Forces			
		F_A	M_A	F_B	M_B
δ_A	Both ends fixed	$-12\frac{EI}{L^3}$	$-6\frac{EI}{L^2}$	$12\frac{EI}{L^3}$	$-6\frac{EI}{L^2}$
m_A		$-6\frac{EI}{L^2}$	$-4\frac{EI}{L}$	$6\frac{EI}{L^2}$	$-2\frac{EI}{L}$
δ_B		$12\frac{EI}{L^3}$	$6\frac{EI}{L^2}$	$-12\frac{EI}{L^3}$	$6\frac{EI}{L^2}$
m_B		$-6\frac{EI}{L^2}$	$-2\frac{EI}{L}$	$6\frac{EI}{L^2}$	$-4\frac{EI}{L}$
δ_A	End A fixed, End B pin-jointed	$-3\frac{EI}{L^3}$	$-3\frac{EI}{L^2}$	$3\frac{EI}{L^3}$	0
m_A		$-3\frac{EI}{L^2}$	$-3\frac{EI}{L}$	$3\frac{EI}{L^2}$	0
δ_B		$3\frac{EI}{L^3}$	$3\frac{EI}{L^2}$	$-3\frac{EI}{L^3}$	0
δ_A	Both ends pin-jointed	0	0	0	0
δ_B		0	0	0	0

Sign convention
Forces on constraints

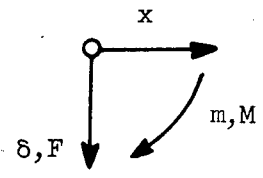

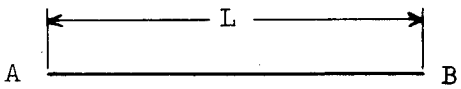

TABLE VIII

BEAM-COLUMN INFLUENCE COEFFICIENTS

[Tension]

Displacement	Unit	Forces (1)			
		F_A	M_A	F_B	M_B
δ_A	Both ends fixed	$-P\frac{ks'}{D_1'}$	$-P\frac{(c'-1)}{D_1'}$	$P\frac{ks'}{D_1'}$	$-P\frac{(c'-1)}{D_1'}$
m_A		$-P\frac{(c'-1)}{D_1'}$	$-\frac{P}{k}\left(\frac{kLc'-s'}{D_1'}\right)$	$P\frac{(c'-1)}{D_1'}$	$-\frac{P}{k}\left(\frac{s'-kL}{D_1'}\right)$
δ_B		$P\frac{ks'}{D_1'}$	$P\frac{(c'-1)}{D_1'}$	$-P\frac{ks'}{D_1'}$	$P\frac{(c'-1)}{D_1'}$
m_B		$-P\frac{(c'-1)}{D_1'}$	$-\frac{P}{k}\left(\frac{s'-kL}{D_1'}\right)$	$P\frac{(c'-1)}{D_1'}$	$-\frac{P}{k}\left(\frac{kLc'-s'}{D_1'}\right)$
δ_A	End A fixed	$-P\frac{k}{t'D_2'}$	$-P\frac{1}{D_2'}$	$P\frac{k}{t'D_2'}$	0
m_A	End B pin-jointed	$-P\frac{1}{D_2'}$	$-P\frac{L}{D_2'}$	$P\frac{1}{D_2'}$	0
δ_B		$P\frac{k}{t'D_2'}$	$P\frac{1}{D_2'}$	$-P\frac{k}{t'D_2'}$	0
δ_A	Both ends pin-jointed	$-\frac{P}{L}$	0	$\frac{P}{L}$	0
δ_B		$\frac{P}{L}$	0	$-\frac{P}{L}$	0

[1] $D_1' = 2(1 - c') + kLs'$
$D_2' = (kL/t) - 1$
$k^2 = P/EI$

$s' = \sinh kL$
$c' = \cosh kL$
$t' = \tanh kL$

Sign convention
Forces on constraints

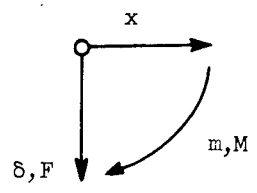

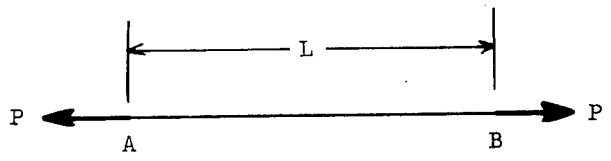

P, positive as shown

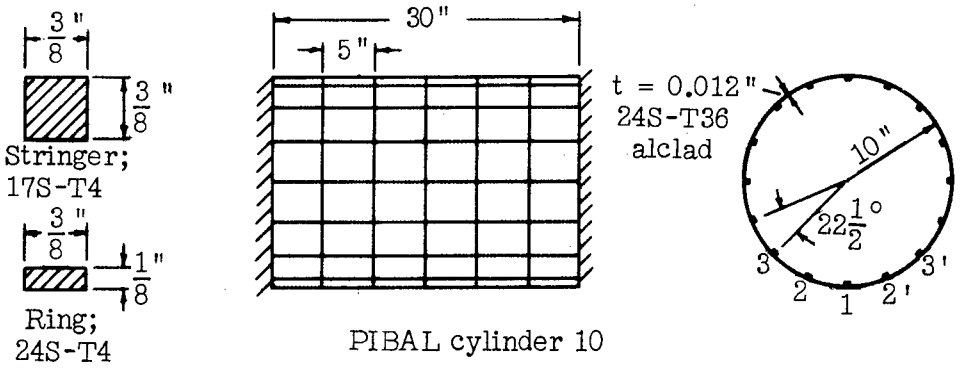

PIBAL cylinder 10

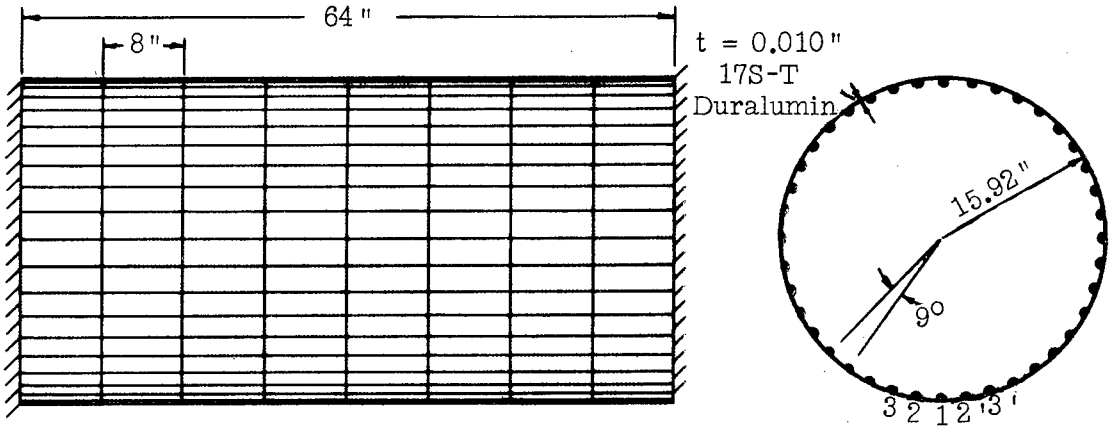

GALCIT cylinder 25

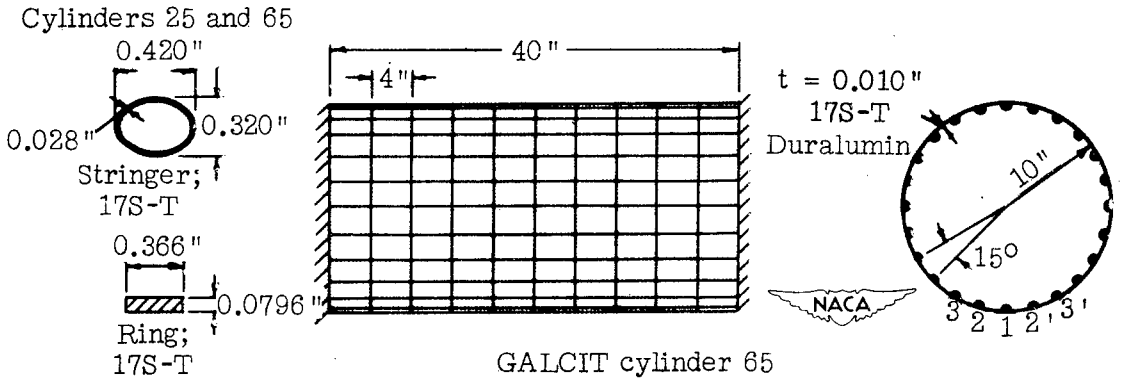

GALCIT cylinder 65

Figure 1.- Cylinder characteristics.

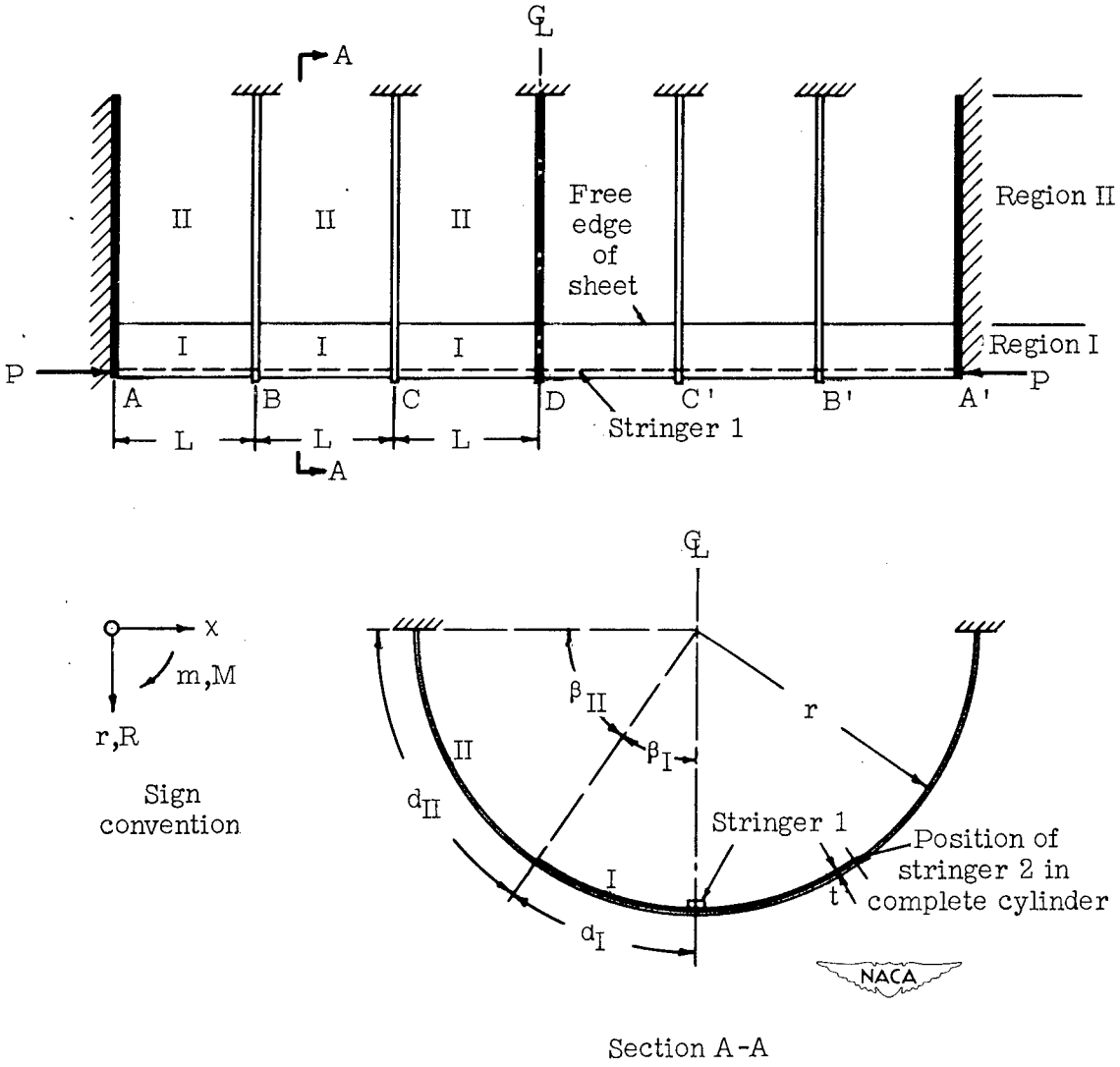

Section A-A

Figure 2.- Simplified structure for setup of operations tables.

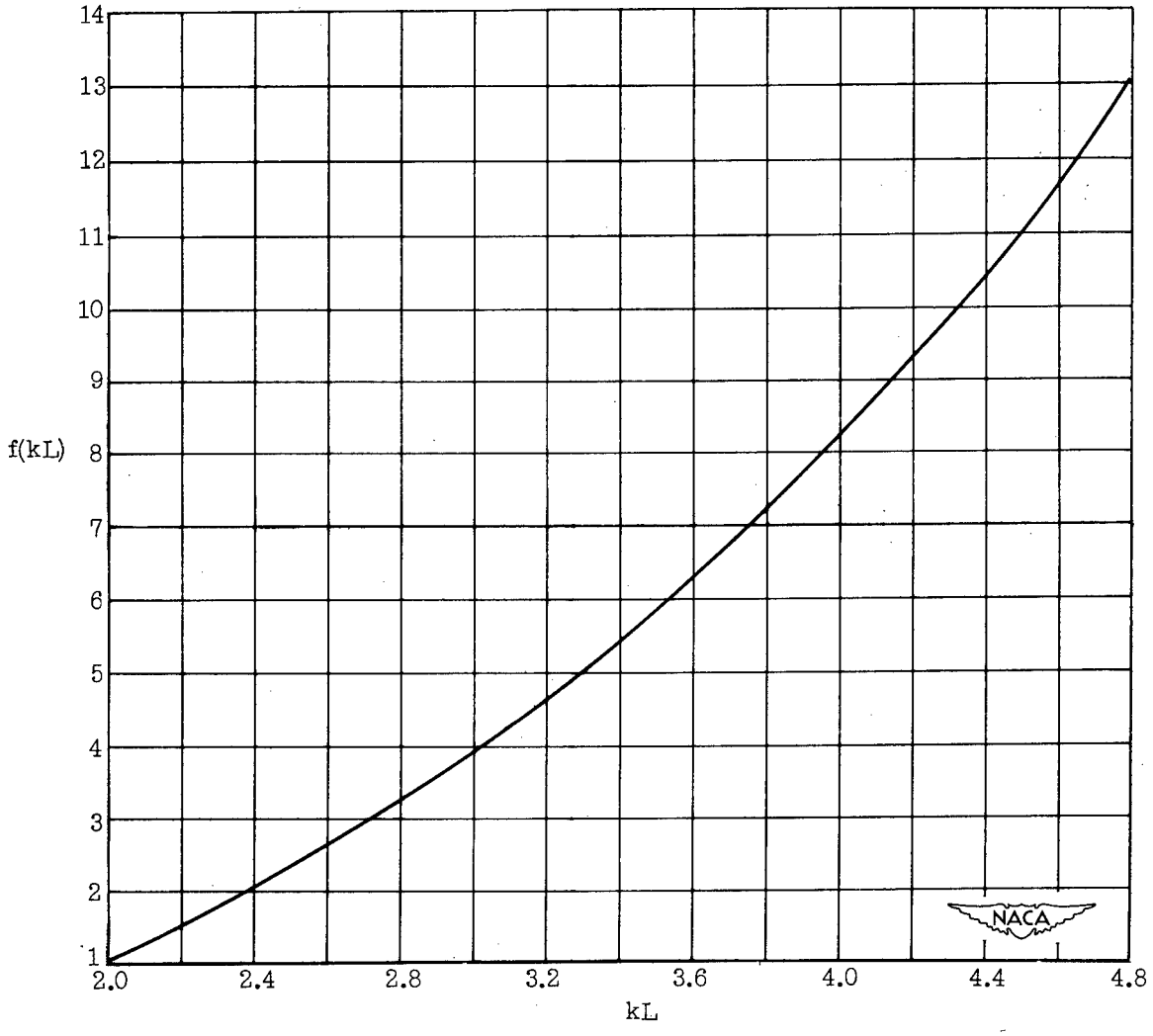

Figure 3.- Plot of f(kL) against kL. $f(kL) = \frac{(kL)^2}{D_1}\left(-0.91592\frac{\sin kL}{kL} - 0.44020\cos kL - 0.47180kL\sin kL + 1.3561\right)$.

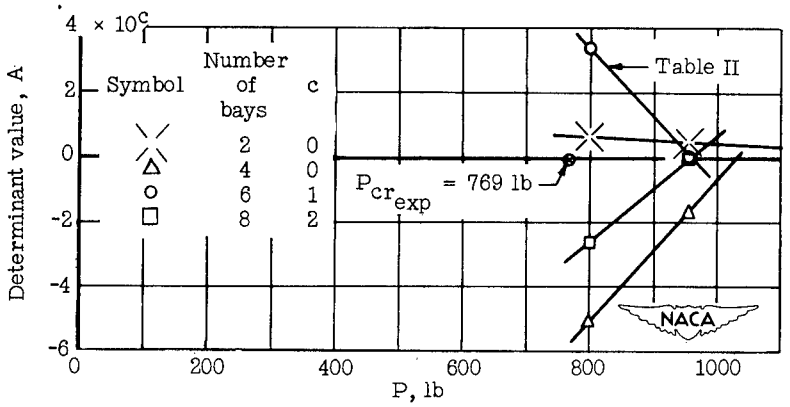

Figure 4.- Determination of buckling load of GALCIT cylinder 25 for two, four, six, and eight bays.

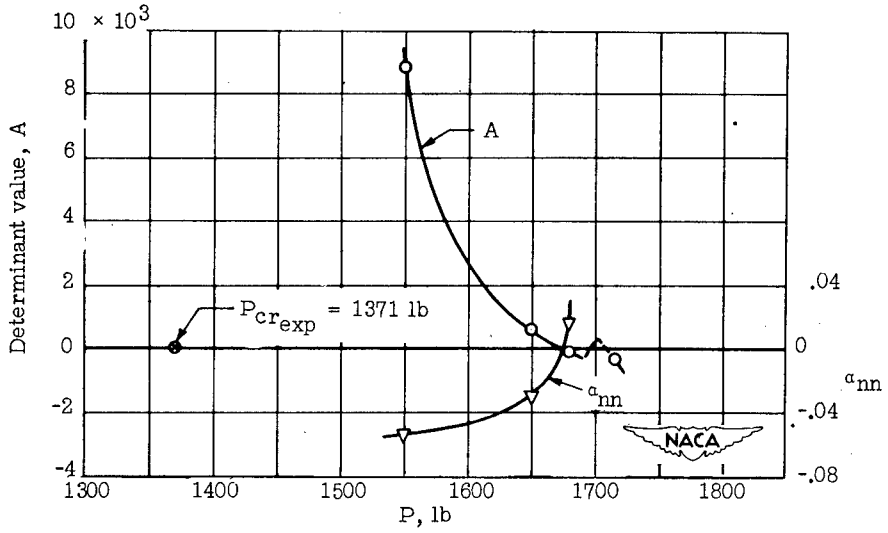

Figure 5.- Determination of buckling load of GALCIT cylinder 65 by table II.

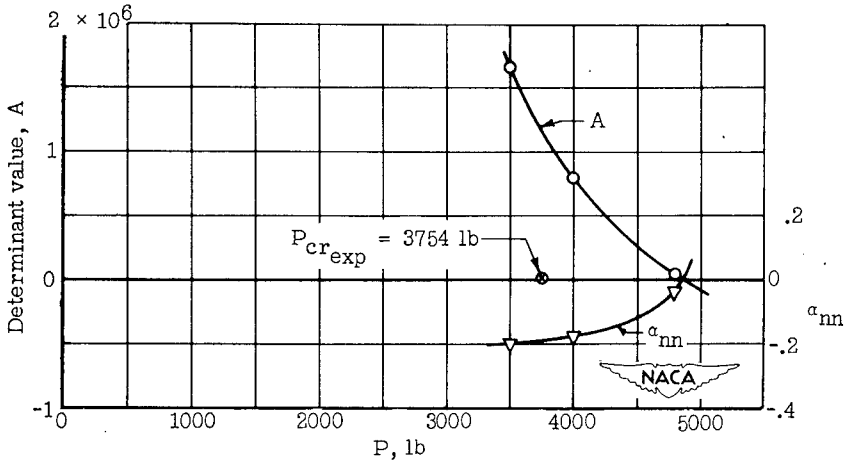

Figure 6.- Determination of buckling load of PIBAL cylinder 10 by table II.

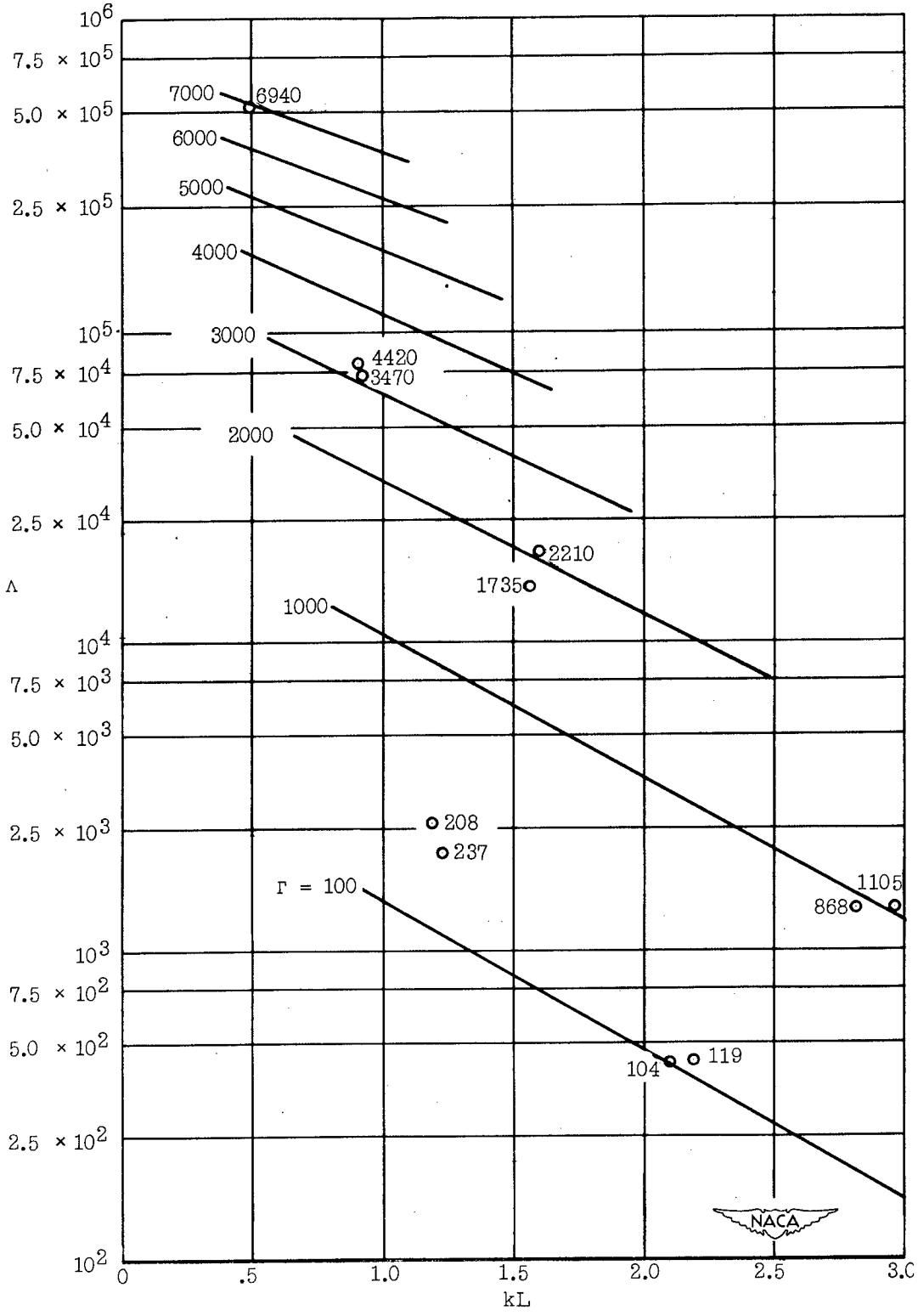

Figure 7.- Experimental variation of kL with parameters Λ and Γ. r/d = 6.32. Value of Γ given for plotted points.

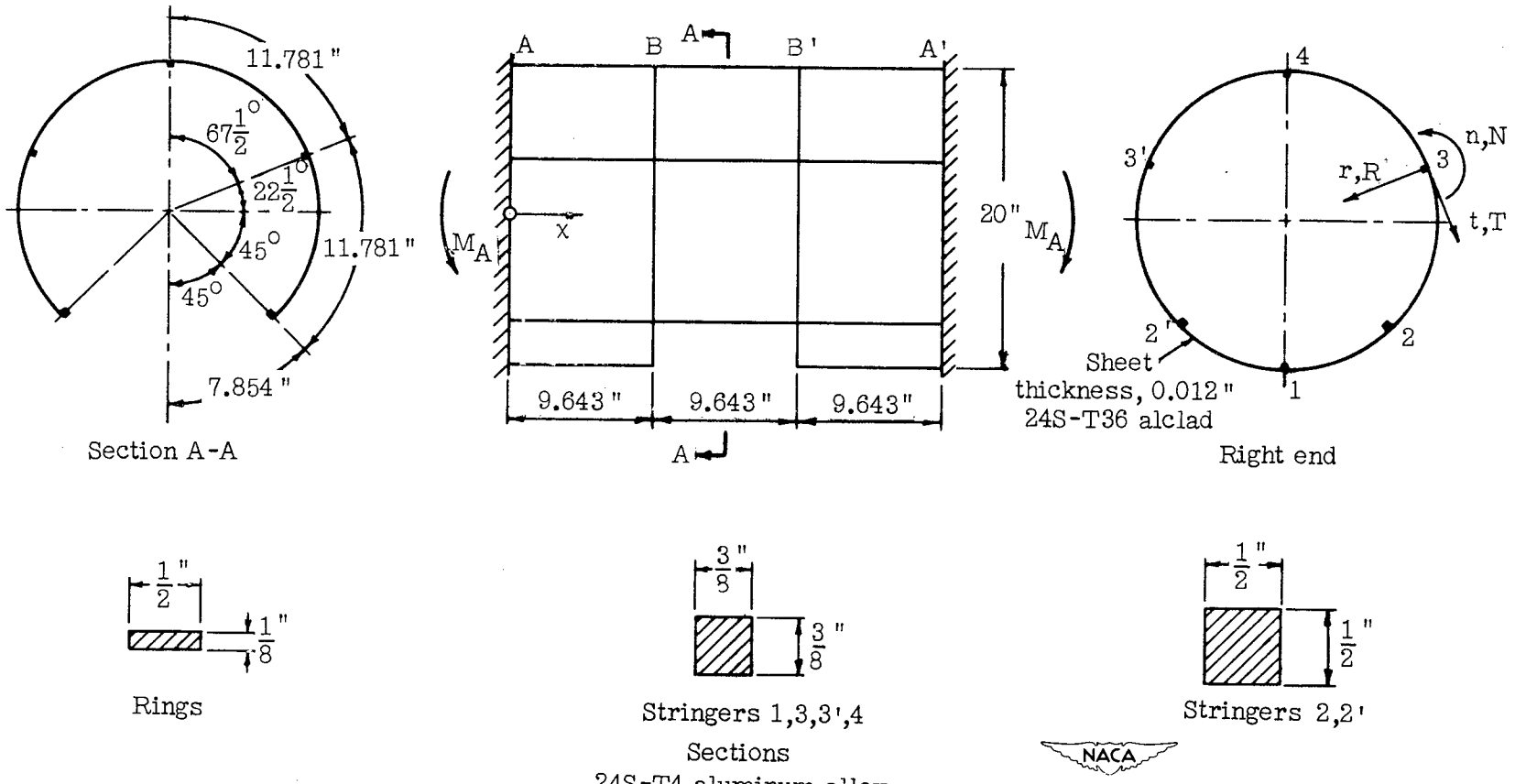

Figure 8.- PIBAL cylinder 82.

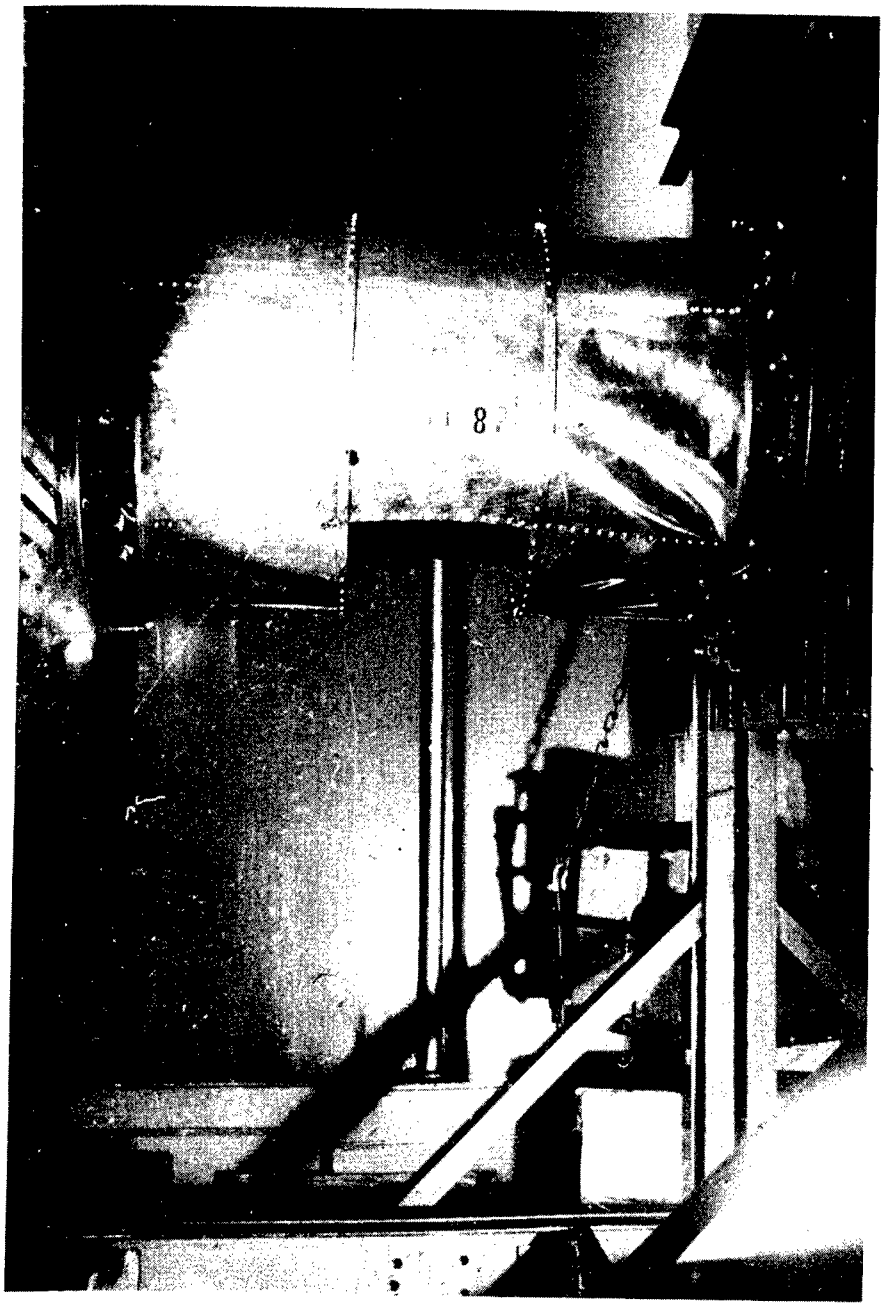

Figure 9.- Side view of PIBAL cylinder 82 after buckling.

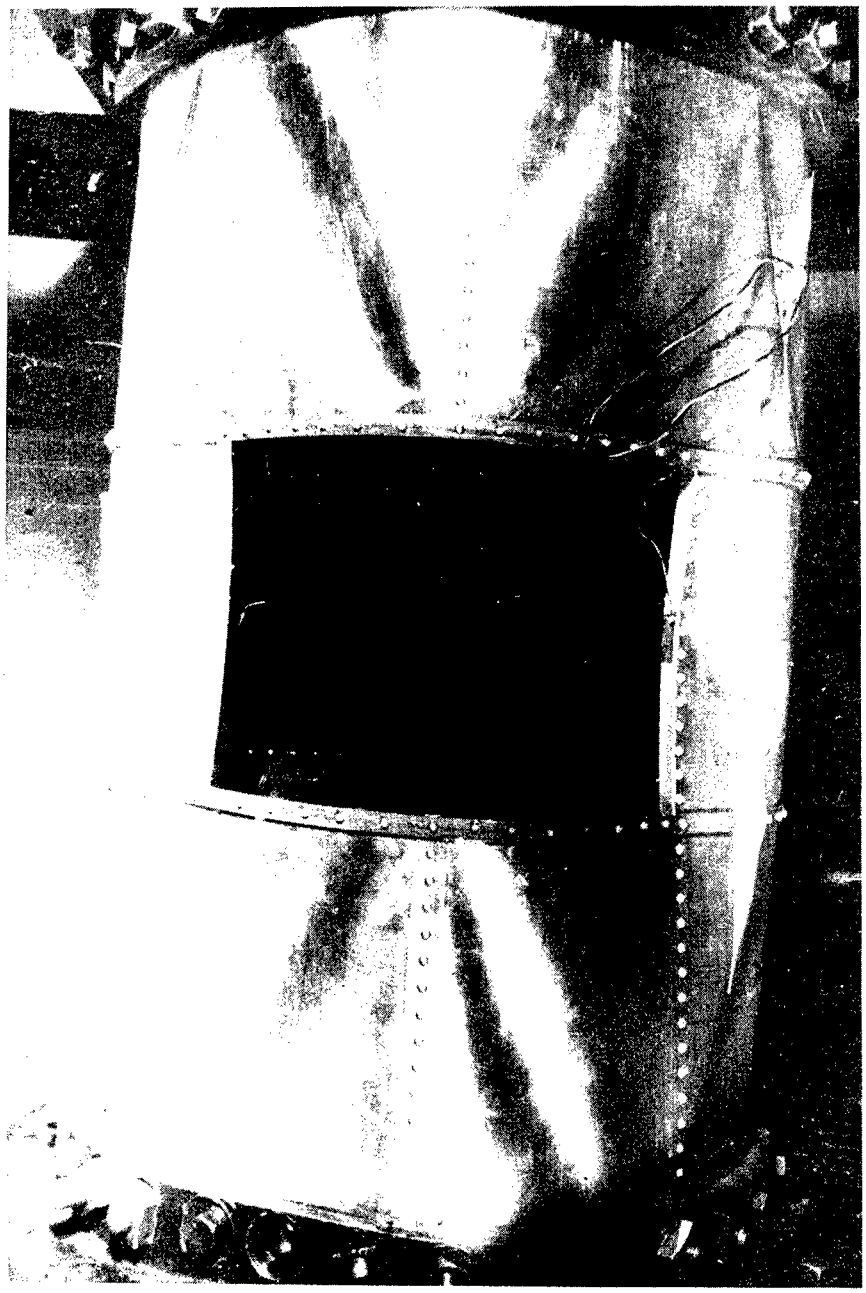

Figure 10.- Bottom view of PIBAL cylinder 82 after buckling.

NACA-Langley - 4-25-51 -1000